

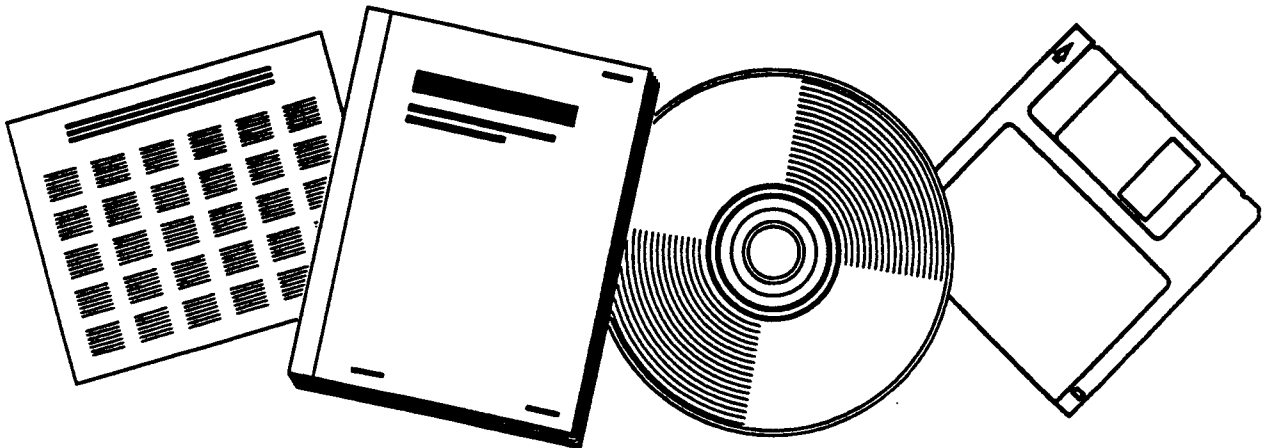


PB98-105398

NTIS[®]
Information is our business.

SCANNING ELECTRON MICROSCOPE STUDIES OF SILICA FUME CONCRETE

FEB 97



U.S. DEPARTMENT OF COMMERCE
National Technical Information Service

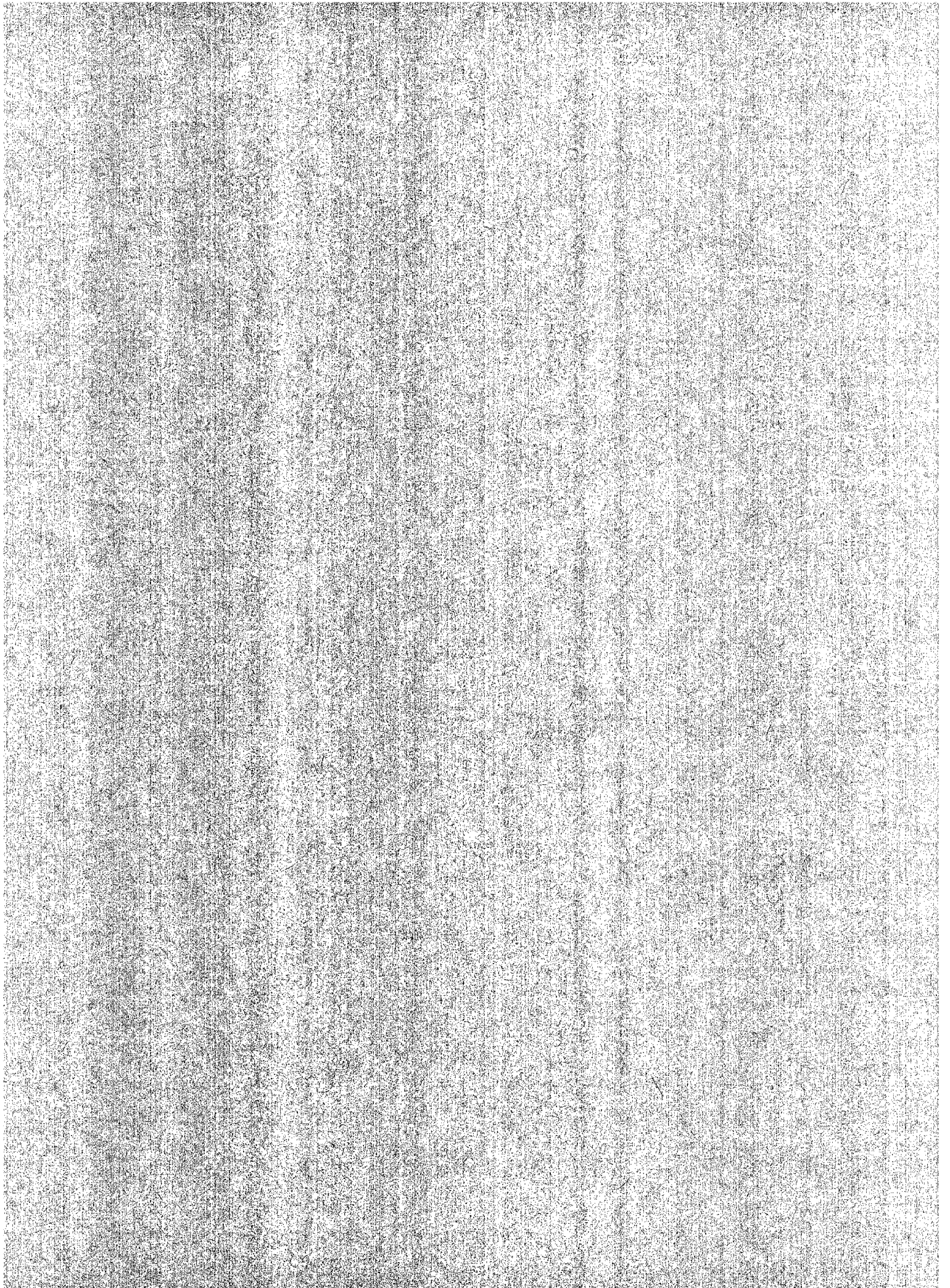


PB98-105398

SCANNING ELECTRON MICROSCOPE STUDY OF FIBER REINFORCED CONCRETE

REPRODUCED BY: **NTIS**
U.S. Department of Commerce
National Technical Information Service
Springfield, Virginia 22161

PROGRAM BETWEEN



**K-TRAN PROJECT KSU 93-4
SCANNING ELECTRON MICROSCOPE STUDIES OF SILICA FUME CONCRETE**

Final Report

Prepared

for

**Kansas Department of Transportation
2300 Van Buren
Topeka, Kansas 66611-1195**

by

S. T. Chou and L. T. Fan

**Department of Chemical Engineering
Durland Hall
Kansas State University
Manhattan, Kansas 66506**

February 1997

1. Report No. KTRAN KSU-93-4	2 PB98-105398 	3. Recipient Catalog No.	
4. Title and Subtitle Scanning Electron Microscope Studies of Siliica Fume Concrete		5. Report Date Feb 1997	
		6. Performing Org. Code	
7. Author(s) S. T. Chou and L. T. Fan		8. Performing Org. Report No.	
9. Performing Organization Name and Address Kansas State University Department of Chemical Engineering Manhattan, Kansas 66506		10. Work Unit No. (TRAIS)	
		11. Contract or Grant No. KSU-93-4 (C-298)	
12. Sponsoring Agency Name and Address Kansas Department of Transportation Docking State Office Bldg. Topeka, Kansas 66612		13. Type of Report and Period Covered Final Report July 1992 to Feb 1997	
		14. Sponsoring Agency Code 106 RE-0008-01	
15. Supplementary Notes			
<p>16. Abstract</p> <p>Six series of experiments were carried out focusing on the effects of silica fume content ranging from 0 to 100 percent with and without chemical admixtures on the strengths of cement-silica fume mixes and on the characterization of the resultant paste or mortar with Scanning Electron Microscope (SEM), X-Ray Defractometer (XRD) and Energy Dispersive Spectroscope (EDS).</p> <p>For cement-silica fume paste, the samples with 2.5% silica fume by weight and without superplasticizer gained the highest strength at 28 days. With the addition of superplasticizer, the samples required less water to maintain a desirable slump, resulting in moderate increases in compressive strength compared to those without, and the gain in strength was highest at 5.0% silica fume.</p> <p>For cement-silica fume mortar, the samples with 7.5% silica fume and with or without superplasticizer gained the highest strength at 28 days. The reduction of water when adding the superplasticizer did not increase the compressive strength of the cement-silica fume mortar as anticipated.</p> <p>No significant differences in the appearance were observed while scanning the surfaces of the samples of cement-silica fume paste at magnifications of 100X and 3000X. Gel-like calcium silica hydrate was observed covering the cement and sand grains in the cement-silica fume mortar. Needle-like ettringite and crystalline calcium hydroxide were also observed in these samples.</p> <p>The major compounds identified in the cement-silica fume paste samples using XRD included SiO₂, Ca(OH)₂, 2CaO.Fe₂O₃, 2CaO-SiO₂, 2CaO-SiO₂.H₂O, 3CaO.Al₂O₃.3CaSO₄.3H₂O, 4CaO.Al₂O₃.13H₂O and 6CaO.4SiO₂.3H₂O. Compound SiO₂ was the only component identified in the pure silica fume sample, indicating no hydration took place.</p> <p>The elements identified in the cement-silica fume paste samples using EDS included Al, Ca, Fe, K, Ma, S and Si. No correlation could be discerned between the Ca/Si ratio and the compressive strength of the samples.</p>			
17. Key Words Cement, silica fume, mortar, scanning electron microscope (SEM), energy dispersive spectroscope (EDS), X-ray defractometer (XRD), superplasticizer, compressive strength.		18. Distribution Statement No restrictions. This document is available to the public through the National Technical Information Service, Springfield, VA 22161	
19. Security Classification (of this Report) Unclassified	20. Security Classification (of this page) Unclassified	21. No. of Pages 100	22. Price

PREFACE

This research project was funded by the Kansas Department of Transportation K-TRAN research program. The Kansas Transportation Research and New-Developments (K-TRAN) Research Program is an ongoing, cooperative and comprehensive research program addressing transportation needs of the State of Kansas utilizing academic and research resources from the Kansas Department of Transportation, Kansas State University and the University of Kansas. The projects included in the research program are jointly developed by transportation professionals in KDOT and the universities.

NOTICE

The authors and the State of Kansas do not endorse products or manufacturers. Trade and manufacturers names appear herein solely because they are considered essential to the object of this report.

This information is available in alternative accessible formats. To obtain an alternative format, contact the Kansas Department of Transportation, Office of Public Information, 7th Floor, Docking State Office Building, Topeka, Kansas, 66612-1568 or phone (913)296-3585 (Voice) (TDD).

DISCLAIMER

The contents of this report reflect the views of the authors who are responsible for the facts and accuracy of the data presented herein. The contents do not necessarily reflect the views or the policies of the State of Kansas. This report does not constitute a standard, specification or regulation.

TABLE OF CONTENTS

COVER PAGE	i
TABLE OF CONTENTS	ii
LIST OF TABLES	iv
LIST OF FIGURES	v
TECHNICAL SUMMARY	1
INTRODUCTION	3
LITERATURE REVIEW	6
Pozzolanic Reaction Process	6
Mechanisms of Strength Enhancement	10
Pore-size refinement and matrix densification	10
Reduction in content of CH	13
Cement-paste aggregate interfacial refinement	14
Non-pozzolanic Activities	15
EXPERIMENT	17
Materials	17
Equipment	18
Blender	18
Mold	18
Capping device	18
Compressive strength tester	18
X-ray diffractometer (XRD)	18
Scanning electron microscope (SEM)	18
Energy dispersive spectroscopy (EDS)	19
Procedure	19
Blending	19
Casting and curing	20
Unconfined compressive strength test	20
SEM analysis	20
XRD analysis	20
EDS analysis	20
RESULTS AND DISCUSSION	21
Effect of Silica Fume Content on the Performance of Cement-Silica Fume Paste	23
Effect of Chemical Admixture on the Performance of Cement-Silica Fume Paste	23

Effect of Silica Fume Content on the Performance of Cement-Silica Fume Mortar	24
Effect of Chemical Admixture on the Performance of Cement-Silica Fume Mortar	24
SEM Analysis	25
XRD Analysis	26
EDS Analysis	27
CONCLUDING REMARKS	28
REFERENCES	30

LIST OF TABLES

Table 1.	Chemical Composition of Silica Fumes from Silicon Furnace in Norway and North America	33
Table 2.	Mix Designs for Preparing Samples SW-A through SW-J of Cement-Silica Fume Paste	34
Table 3.	Mix Designs for Preparing Samples SW-AA through SW-GG of Cement-Silica Fume Paste	34
Table 4.	Mix Designs for Preparing Samples SW-AA1 through SW-GG1 of Cement-Silica Fume Paste	35
Table 5.	Mix Designs for Preparing Samples SW-A0 through SW-G0 of Cement-Silica Fume Mortar	35
Table 6.	Mix Designs for Preparing Samples SW-A1 through SW-G1 of Cement-Silica Fume Mortar	36
Table 7.	Mix Designs for Preparing Samples S-1 through S-7 of Cement-Silica Fume Paste	36
Table 8a.	Compressive Strengths of Samples of Cement-Silica Fume Paste: SW-A through SW-E	37
Table 8b.	Compressive Strengths of Samples of Cement-Silica Fume Paste: SW-F through SW-J	37
Table 9.	Compressive Strengths of Samples of Cement-Silica Fume Paste: SW-AA through SW-GG	37
Table 10.	Compressive Strengths of Samples of Cement-Silica Fume Paste: SW-AA1 through SW-GG1	38
Table 11.	Compressive Strengths of Samples of Cement-Silica Fume Mortar: SW-A0 through SW-G0	38
Table 12.	Compressive Strengths of Samples of Cement-Silica Fume Mortar: SW-A1 through SW-G1	38

LIST OF FIGURES

Figure 1.	Generation of silica fume as a by-product in the production of silicon metal.	39
Figure 2.	Particle-size distribution of silica fume from a Canadian plant	40
Figure 3.	Blender	41
Figure 4.	Mold	42
Figure 5.	Miniature capping device	43
Figure 6.	Compressive strength tester	44
Figure 7a.	Compressive strengths of samples of cement-silica fume paste: SW-A through SW-E	45
Figure 7b.	Compressive strengths of samples of cement-silica fume paste: SW-F through SW-J	46
Figure 8.	Compressive strengths of samples of cement-silica fume paste: SW-AA through SW-GG	47
Figure 9.	Compressive strengths of samples of cement-silica fume paste: SW-AA1 through SW-GG1	48
Figure 10.	Compressive strengths of samples of cement-silica fume mortar: SW-A0 through SW-G0	49
Figure 11.	Compressive strengths of samples of cement-silica fume mortar: SW-A1 through SW-G1	50
Figure 12a	SEM micrographs of samples of cement-silica fume paste (100X): (i) SW-AA; (ii) SW-BB; (iii) SW-CC; and (iv) SW-DD	51
Figure 12b	SEM micrographs of samples of cement-silica fume paste (100X): (v) SW-EE; (vi) SW-FF; and (vii) SW-GG.	52
Figure 13a.	SEM micrographs of samples of cement-silica fume paste (3,000X): (i) SW-AA; (ii) SW-BB; (iii) SW-CC; and (iv) SW-DD	53

Figure 13b. SEM micrographs of samples of cement-silica fume paste (3,000X): (v) SW-EE; (vi) SW-FF; and (vii) SW-GG	54
Figure 14a. SEM micrographs of samples of cement-silica fume mortar (100X): (i) SW-A0; (ii) SW-B0; (iii) SW-C0; and (iv) SW-D0	55
Figure 14b. SEM micrographs of samples of cement-silica fume mortar (100X): (v) SW-E0; (vi) SW-F0; and (vii) SW-G0	56
Figure 15a. SEM micrographs of samples of cement-silica fume mortar (3,000X): (i) SW-A0; (ii) SW-B0; (iii) SW-C0; and (iv) SW-D0	57
Figure 15b. SEM micrographs of samples of cement-silica fume mortar (3,000X): (v) SW-E0; (vi) SW-F0; and (vii) SW-G0	58
Figure 16a. SEM micrograph of sample S-1 of cement-silica fume paste (10,000X): Area 1	59
Figure 16b. SEM micrograph of sample S-1 of cement-silica fume paste (10,000X): Area 2	60
Figure 16c. SEM micrograph of sample S-1 of cement-silica fume paste (10,000X): Area 3	61
Figure 17a. SEM micrograph of sample S-2 of cement-silica fume paste (10,000X): Area 1	62
Figure 17b. SEM micrograph of sample S-2 of cement-silica fume paste (10,000X): Area 2	63
Figure 17c. SEM micrograph of sample S-2 of cement-silica fume paste (10,000X): Area 3	64
Figure 18a. SEM micrograph of sample S-3 of cement-silica fume paste (10,000X): Area 1	65
Figure 18b. SEM micrograph of sample S-3 of cement-silica fume paste (10,000X): Area 2	66
Figure 18c. SEM micrograph of sample S-3 of cement-silica fume paste (10,000X): Area 3	67

Figure 19a.	SEM micrograph of sample S-4 of cement-silica fume paste (10,000X): Area 1	68
Figure 19b.	SEM micrograph of sample S-4 of cement-silica fume paste (10,000X): Area 2	69
Figure 19c.	SEM micrograph of sample S-4 of cement-silica fume paste (10,000X): Area 3	70
Figure 20a.	SEM micrograph of sample S-5 of cement-silica fume paste (10,000X): Area 1	71
Figure 20b.	SEM micrograph of sample S-5 of cement-silica fume paste (10,000X): Area 2	72
Figure 20c.	SEM micrograph of sample S-5 of cement-silica fume paste (10,000X): Area 3	73
Figure 21a.	SEM micrograph of sample S-6 of cement-silica fume paste (10,000X): Area 1	74
Figure 21b.	SEM micrograph of sample S-6 of cement-silica fume paste (10,000X): Area 2	75
Figure 21c.	SEM micrograph of sample S-6 of cement-silica fume paste (10,000X): Area 3	76
Figure 22a.	SEM micrograph of sample S-7 of cement-silica fume paste (10,000X): Area 1	77
Figure 22b.	SEM micrograph of sample S-7 of cement-silica fume paste (10,000X): Area 2	78
Figure 22c.	SEM micrograph of sample S-7 of cement-silica fume paste (10,000X): Area 3	79
Figure 23.	XRD pattern of sample S-1 of cement-silica fume paste	80
Figure 24.	XRD pattern of sample S-2 of cement-silica fume paste	81
Figure 25.	XRD pattern of sample S-3 of cement-silica fume paste	82
Figure 26.	XRD pattern of sample S-4 of cement-silica fume paste	83

Figure 27.	XRD pattern of sample S-5 of cement-silica fume paste	84
Figure 28.	XRD pattern of sample S-6 of cement-silica fume paste	85
Figure 29.	XRD pattern of sample S-7 of cement-silica fume paste	86
Figure 30.	EDS spectrum of sample S-1 of cement-silica fume paste	87
Figure 31.	EDS spectrum of sample S-2 of cement-silica fume paste	88
Figure 32.	EDS spectrum of sample S-3 of cement-silica fume paste	89
Figure 33.	EDS spectrum of sample S-4 of cement-silica fume paste	90
Figure 34.	EDS spectrum of sample S-5 of cement-silica fume paste	91
Figure 35.	EDS spectrum of sample S-6 of cement-silica fume paste	92
Figure 36.	EDS spectrum of sample S-7 of cement-silica fume paste	93

TECHNICAL SUMMARY

Numerous studies have been undertaken since 1976 to investigate the effects of silica fume on the performance of concrete. The addition of silica fume to portland cement paste, mortar or concrete improves the strengths of the mixtures. Three mechanisms have been proposed for this phenomenon. They are: (1) pore-size refinement and matrix densification, (2) reduction in the content of calcium hydroxide, and (3) cement-paste-aggregate interfacial refinement. The objectives of this research are: (i) to observe the progress of mineralization (hydration) in concrete containing silica fume; (ii) to correlate mix specifications and test results to the silica-fume content.

To avoid duplication of past work as well as to reduce the number of factors affecting the performance of concrete, six series of experiments were carried out in the present study focusing only on the effects of silica-fume content from 0 to 100 percent with and without chemical admixtures on the strengths of cement-silica fume mixes and on the characterization of the resultant paste or mortar with SEM, XRD, and EDS.

The following significant results were obtained:

1. For cement-silica fume paste, the samples with a silica fume replacement of around 2.5 wt% and without superplasticizer gained the highest strength at 28 days. With the addition of the superplasticizer, the samples required less water to maintain a desirable slump, thereby resulting generally in moderate increases in the compressive strength compared to those without, and the gain in the strength was highest at a silica fume replacement of 5.0 wt% instead of 2.5 wt%.

2. For cement-silica fume mortar, the samples with a silica fume replacement of approximately 7.5 wt% and with and/or without superplasticizer gained the highest strength at 28 days. The reduction of water by adding superplasticizer in the mortar containing silica fume did not increase the compressive strengths of the samples of cement-silica fume mortar as anticipated.

3. No significant differences in the appearance were observed while scanning the surfaces of the samples of cement-silica fume paste with various silica fume contents at magnifications of 100X and 3,000X. Gel-like calcium silica hydrate was, however, observed covering the cement and the sand grains in the cement-silica fume mortar. Needle-like ettringite and crystalline calcium hydroxide were also observed in these samples.

4. The major compounds identified in the samples of cement-silica fume paste by the XRD included SiO_2 , Ca(OH)_2 , $2\text{CaO}\cdot\text{Fe}_2\text{O}_3$, $2\text{CaO}\cdot\text{SiO}_2$, $2\text{CaO}\cdot\text{SiO}_2\cdot\text{H}_2\text{O}$, $3\text{CaO}\cdot\text{Al}_2\text{O}_3\cdot3\text{CaSO}_4\cdot31\text{H}_2\text{O}$, $4\text{CaO}\cdot\text{Al}_2\text{O}_3\cdot13\text{H}_2\text{O}$, and $6\text{CaO}\cdot4\text{SiO}_2\cdot3\text{H}_2\text{O}$. Compound SiO_2 was the only component identified in the sample of pure silica fume, thereby indicating that no hydration took place in this sample.

5. The elements identified in the samples of cement-silica fume paste by the EDS included Al, Ca, Fe, K, Mg, S, and Si. No correlation, however, could be discerned between the Ca/Si ratio and the compressive strength of the samples.

INTRODUCTION

In recent years, many commercial entities and public agencies have become increasingly involved in research aimed at waste utilization and energy conservation in cement and concrete industries. In part, this is being accomplished by promoting the use of cementitious materials such as fly ash and slag. Lately, some attention has been given to partial replacement of cement with condensed silica fume because of the increased production of this material as well as the strict enforcement of pollution control measures to prevent dispersion of the material into the atmosphere. Furthermore, the availability of superplasticizers has generated new possibilities for the application of silica fume as a supplementary cementing material.

Silica fume is a by-product from the production of silicon metal or ferrosilicon alloys in electric arc furnaces. Reduction of quartzic silica in the presence of carbon at temperatures around 2,000 °C results in the production of silicon; see Figure 1. About 10 to 15% of the quartz is lost in the form of SiO_2 . The fume is collected by filtering the gases escaping from the furnaces. After cooling, the gases condense into extremely small spheres of amorphous SiO_2 (see, e.g., Mehta, 1983). Silica fume has been variously called silica dust, condensed silica fume, and silica powder.

Silica fume varies from light to dark gray in color and yields a black slurry when mixed with water. The specific gravity of a typical silica fume is approximately 2.2 compared to 3.2 for normal portland cement. The uncompacted unit weight (bulk density) of silica fume ranges approximately from 250 to 300 kg/m^3 whereas that of normal portland cement is approximately 1,200 kg/m^3 . Silica fume consists of inordinately fine vitreous particles with a spheric surface area of about 20,000 m^2/kg . Its extreme fineness is best illustrated by the following comparison with other fine materials (Malhotra and

Carette, 1983):

Silica fume	:	20,000 m ² /kg
Tobacco smoke	:	10,000 m ² /kg
Fly ash	:	400 to 700 m ² /kg
Normal portland cement	:	300 to 400 m ² /kg

The particle-size distribution of a typical silica fume shows that most particles are smaller than 1 μm with an average diameter of approximately 0.1 μm ; see Figure 2 (Malhotra and Carette, 1983).

Table 1 lists a typical chemical composition of silica fume produced in North America (Mehta and Gjorv, 1982). For comparison, it also lists the chemical compositions of typical silica fumes from silicon furnaces in Norway. The fumes generally contain more than 90% of silicon dioxide, most of which is amorphous in form. The chemical compositions of the fumes vary according to the type of alloy or metal being produced from electric furnaces. For example, the fumes from a ferrosilicon furnace will generally contain more iron and magnesium than those from a furnace producing silicon metal.

Partial replacement of portland cement with silica fume in mortar and concrete has been practiced for decades. It can be either blended with cement or added as the concrete is batched. Typically, it results in an increase in compressive and flexural strength. Applications of silica fume in North America have been widely reported (see, e.g., Buck and Burkes, 1981; Holland and Gutschow, 1987; Cohen and Olek, 1989; Cohen *et al.*, 1991; Durning and Hicks, 1991; Detwiler, 1992; Luther, 1993). Bache (1981) and Wolsiefer (1982) produced ultra high-strength concrete with a compressive strength ranging from 18,000 to 38,900 psi with the addition of silica fume and superplasticizers. Like fly ash and natural pozzolan, silica fume has been used to control alkali-silica reactions in concrete with the additional advantage that smaller quantities are needed than

fly ash and natural pozzolan (Oberholster and Westra, 1981). It has been shown that the incorporation of silica fume can improve the early-age strength of fly ash/portland cement concrete (Mehta and Gjord, 1982). Lessard *et al.* (1982) and Berke *et al.* (1988) have reported that the chloride-ion permeability of silica fume concrete is much lower than that of non-silica fume concrete. According to Aitcin and Vezina (1984), the resistance to freezing and thawing of silica fume concrete is far superior to plain or regular concrete.

The State of Kansas is routinely using silica fume concrete in bridge deck overlays. Concrete has the promise of increasing deck durability by reducing the permeability of the overlay. The mechanisms involved in the reaction of silica fume are complex and not well defined. The objectives of this research are: (i) to observe the progress of mineralization (hydration) in concrete containing silica fume; (ii) to correlate mix specifications and test results to the silica-fume content.

LITERATURE REVIEW

The performance of silica fume in concrete has been investigated in Scandinavian countries, particularly in Norway and Denmark where the material has been employed on a limited scale since 1976 (Traetteberg, 1978; Jahr, 1980). The improvement in the strength of concrete through the addition of silica fume is mainly attributable to the pozzolanic reaction between the silica fume particles and Ca(OH)_2 generated from the hydration of portland cement. The mechanisms of such a reaction, however, are highly complex and are only partially understood.

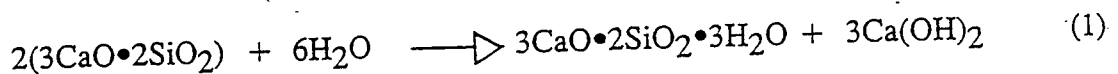
Pozzolanic Reaction Process

Pozzolans are siliceous, aluminous, and ferric material, which, in the presence of moisture and at room temperature, can react with Ca(OH)_2 (or CH) to form products, calcium silicate hydrates (or C-S-H), calcium aluminate hydrates (or C-A-H), and calcium sulphoaluminate hydrates (or C-S̄-A-H); these products contribute to the strength of concrete (see, e.g., Mehta, 1983). The CH is one of the products of hydration of portland cement and constitutes about 20%, by volume, of the hydration product (see, e.g., Mehta, 1983).

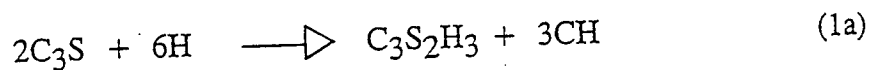
Colloidal silica, 0.0005 to 0.5 μm in size, or similar materials behave like pozzolans; their pozzolanic nature is now well established. Usually, the percentage of CH consumed by silica fume has served as an index of the pozzolanic activity of silica fume. Contradictory data have been obtained with respect to the percentage of CH consumed by silica fume. Traetteberg (1978), one of the first to study silica fume, reported that only about 2% of the liberated CH was consumed by silica fume in a portland cement paste containing 10% silica fume by weight of cement. In contrast, Buck and Burkes (1981)

reported high pozzolanic activity in portland cement-silica fume pastes in which all the CH liberated was consumed by silica fume approximately at 28 days. Sellevold *et al.* (1981) have studied pastes of cement with silica fume by X-ray diffraction quantitative analysis (QXRD), thermogravimetric analysis (TGA), mercury porosimetry, and other methods. According to their results, the addition of 24% silica fume by weight of cement is sufficient to consume all the CH, thereby indicating that silica fume involved in the pozzolanic reaction is highly reactive.

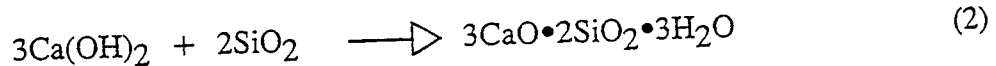
Nelson and Young (1977) studied the pozzolanic activity of colloidal silica added to tricalcium silicate ($3\text{CaO}\cdot\text{SiO}_2$, or C_3S) and portland cement pastes. The colloidal silica contained 99.8% of amorphous SiO_2 , and its surface area ranged from 175,000 to 430,000 m^2/kg . The amorphous silica was added to the C_3S pastes in the amount varying from 25 to 75% of the theoretical value required to convert all the CH to C-S-H according to the following two equations.



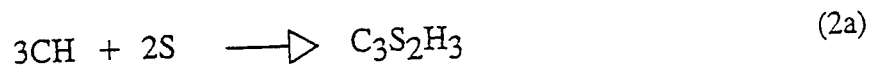
or



and



or



The amount of CH, expressed as a percentage of the weight of the original C_3S , was determined by TGA at different ages. At 3 days, the content of CH was reduced by 14 and 73% when 25 and 75% amorphous silica, respectively, were added to C_3S . Even greater reductions in CH were observed with the portland cement pastes. For example,

with an addition of 25% amorphous silica, the CH content was reduced as much as 65% relative to the control paste after one day's curing. From these results, Nelson and Young (1977) have concluded that amorphous silica of colloidal dimensions is a highly reactive pozzolan and the pozzolanic reaction may occur as early as the first day of curing.

Cheng and Feldman (1985) observed that the hydration in portland cement was accelerated in the presence of silica fume particles because of their reaction with Ca^{2+} ions and their ability to act as nucleation sites for CH. The hydration occurred within minutes after contact with water and the reduced Ca^{2+} ions affected the nature of the hydration products. In the study of Cheng and Feldman (1985), pozzolanic reaction occurred as early as 8 hours after the samples were prepared.

Grutzeck *et al.* (1983) investigated the mechanism of the pozzolanic reaction of silica fume with CH in aqueous solutions; the silica fume, approximately $0.1\mu\text{m}$ in size, had a SiO_2 content of 94% and a surface area of $20,200\text{ m}^2/\text{kg}$. Two experiments were carried out, one at 20°C with 0.33 g of silica fume and the other at 38°C with 0.28 g of silica fume added to 500 ml of aqueous CH solution. Samples were taken from each solution and examined with a scanning electron microscope (SEM). The results have yielded a model for the reactions of silica fume with CH in aqueous solutions. The model envisions the following:

As soon as silica fume comes in contact with water, part of the silica fume undergoes rapid dissolution. After 5 to 15 minutes of mixing, the silica in solution tends to form a coating of amorphous silica-rich, Ca-poor "gel" on the surfaces of the silica fume particles; simultaneously, the silica fume particles agglomerate and form clusters. Nevertheless, this coating begins to dissolve after 1 hr and the silica fume clusters start reacting with CH to form C-S-H. The initial reaction of silica fume to form this "gel" is a rapid

surface-dependent reaction. In contrast, the formation of the C-S-H via the pozzolanic reactions is temperature-dependent. This stems from the fact that the C-S-H becomes abundant approximately at 8 hrs and 38°C as well as at 24 hrs and 20°C.

Grutzeck *et al.* (1983) extended their model to elucidate certain characteristics of portland cement-silica fume paste, mortar, and concrete mixes prepared in their earlier work (Grutzeck *et al.*, 1982). These characteristics include the high water demand, early strength gain, dense micro-structure, and reduction in CH content. Portland cement-silica fume paste was prepared with 69.4% cement, 15.3% silica fume, and 15.3% quartz, with a water/cement (w/c) ratio of 0.43 and a superplasticizer/deionized water rate of 1.4 g/30.2 g. The high water demand and premature hardening of portland cement-silica fume paste were attributed to the absorption of water in forming the silica-rich, Ca-poor "gel". Initially, the "gel" thickened the cement paste, thereby resulting in the early setting of the paste. Later, the "gel" dissolved and the silica-fume particles reacted with CH liberated from the hydration of calcium silicates in the portland cement to form additional C-S-H; this led to the formation of a rigidly cemented C-S-H network. There were, however, some noticeable differences. The reaction was relatively slow for the portland cement-silica fume paste. Agglomeration of the silica-fume particles occurred, but not in all cases. Although C-S-H formed on the surfaces of the agglomerates, it was difficult to distinguish between the C-S-H formed through the pozzolanic reaction of silica-fume particles and that formed by the hydration of the calcium silicates. Despite these differences, it was concluded that the C-S-H model with the assumption of silica-rich, Ca-poor "gel" formation is valid for the hydration of portland cement-silica fume pastes; the model is capable of elucidating the concomitant phenomena observed.

Kurbus *et al.* (1985) studied the reactivity of silica fume with CH in portland cement pastes at 55 and 90 °C. The silica fume had a SiO₂ content of 92.6% and a surface area

of 29,900 m²/kg, and the pastes had a w/c ratio of 0.50. The paste hydration was carried out in closed polyethylene bottles under saturated steam conditions from 2.5 to 24 hrs. Depending on its initial quantity, as much as 68 to 95% of the CH had reacted with silica fume after 2.5 hrs at 90 °C, whereas only 25 to 55% of the CH had reacted with the silica fume after 2.5 hrs at 55 °C. The quantity of unreacted CH was 3 to 8% after 24 hrs, independent of both temperature and initial quantity of CH. The conclusion was that the reactivity of silica fume with CH depends strongly on temperature at early stages, but not later, for example at 24 hrs.

Mechanisms of Strength Enhancement

The addition of silica fume to portland cement paste, mortar or concrete improves the strength of the portland cement mixtures. Three mechanisms have been proposed for this phenomenon; they are discussed in the following subsections.

Pore-size refinement and matrix densification

Mehta (1981) studied the strength development of portland-pozzolan cement pastes. A volcanic ash (Santorin Earth) resembling silica fume with a SiO₂ content of 65% and a surface area of 15,000 m²/kg served as the pozzolanic material. Three samples of portland-pozzolan cement were prepared with 10, 20, and 30% replacement of cement by the pozzolan. The w/c ratio of the pastes was 0.50. Compressive strength tests were performed according to ASTM C-109. In addition, the pore-size distribution was analyzed by a mercury penetration technique. The compressive strength tests showed that at 28 days, the paste containing 10% of pozzolan exhibited the highest strength (6% over the portland cement paste serving as the control). After one year, the paste with 20% pozzolan had the highest strength with an increase of 10% over the control. These strength

characteristics could be elucidated in terms of the pore-size distribution of the hydrated pastes. For example, the highest strength achieved by the paste containing 10% pozzolan at 28 days was attributed to the low volume of large pores ($> 0.1 \mu\text{m}$) present in the paste, whereas the highest strength achieved by the paste with 20% pozzolan after 1 year was attributed to both the absence of the large pores and the large volume of small pores ($< 0.05 \mu\text{m}$) in the paste. From these results, it has been concluded that the volume of large pores, not the total porosity, adversely affects the strength of the hydrated cement pastes. Moreover, the transformation of large pores into finer pores, i.e., pore refinement, induced by the pozzolanic reaction plays an important role in enhancing the strength of portland-pozzolan cement.

Mehta and Gjory (1982) investigated the strength development of concrete in which 30% of portland cement was replaced by an equal volume of Class F fly ash or silica fume. Compressive strength tests were carried out with 100 mm cube specimens at 3, 7, 28, and 90 days. In addition, the pore-size distribution was analyzed by a mercury penetration technique. The compressive strength of the concrete with fly ash, i.e., cement-fly ash concrete, was lower than the corresponding strength of the concrete serving as the control. For example, the strengths of the cement-fly ash concrete at 7 and 28 days were, respectively, 11 and 12% less than that of the concrete serving as the control; however, the strength of the cement-fly ash concrete at 90 days was similar to the concrete serving as the control. On the other hand, the concrete with silica fume, i.e., cement-silica fume concrete, exhibited much higher strength than the concrete serving as the control, particularly at 7, 28, and 90 days. It was observed that the total volume of large pores ($> 0.1 \mu\text{m}$) was higher for the cement-fly ash pastes than for the cement pastes serving as the control at 7 and 28 days. As a result, the concrete prepared with the portland cement and fly ash (at the same w/c ratio) exhibited lower strengths than the concrete serving as the control at these two ages. At 90 days, however, the volume of large pores was similar,

and consequently, pastes had similar strength even though the total volume of the pores of the fly ash-portland cement paste was much higher than that of the portland cement paste.

At 7 days, the volume of the large pores was only $0.12 \text{ cm}^3/\text{g}$ for the cement-silica fume paste in contrast to $0.30 \text{ cm}^3/\text{g}$ for the cement paste without silica fume. A 22% increase in the strength of the former over the latter may have been attributable to the reduction of the volume of the large pores. Moreover, there were hardly any large pores for the cement-silica fume pastes at 28 and 90 days even though their total pore volumes were similar. In contrast, the volumes of the large pores were $0.22 \text{ cm}^3/\text{g}$ and $0.17 \text{ cm}^3/\text{g}$, respectively, for the cement pastes without silica fume at the same ages. It was observed that the strengths of the portland cement-silica fume concrete were 77 and 97%, respectively, higher than those of the concrete without silica fume at 28 and 90 days. Thus, it has been concluded that the presence of silica fume in the portland cement mixes substantially reduces the volume of large pores at all ages and, therefore, is instrumental in causing the observed increases in compressive strength.

The exact mechanism by which the process of pore refinement takes place in silica fume-portland cement paste is not completely understood. Certain conclusions, however, can be drawn by observing the micro-structure of these pastes.

Regourd *et al.* (1983) studied the micro-structure of blended cement mortars with 30% of various additives, in which one-sixth of the additive (or 5%, based on cement) was replaced by an equal amount of silica fume; the additives were slag, fly ash, volcanic rock and quartz. The micro-structure was examined with an SEM from 7 up to 90 days. The replacement of 5% was found to result in a denser C-S-H with lower microporosity than blended cement mortars without silica fume.

An electron probe microanalysis (EPMA) by Regourd *et al.* (1983) revealed that the CaO to SiO₂ (or C/S) ratio of the C-S-H was lower for the cement mortar with silica fume than without. For example, the C/S ratio for the ordinary portland cement mortars was 1.7, as compared to 1.2 for the mortar with 70% portland cement, 5% silica fume, and 25% slag. The decrease in the calcium content was attributed to the lime consumption mainly by the silica fume, activated by the Ca²⁺ ions liberated by the hydration of the portland cement silicates.

Regourd *et al.* (1982) also investigated the micro-structure in the portland cement-silica fume concrete of a pavement installed in Canada. The content of silica fume ranged from 10 to 40% by the weight of cement. After one winter of service, cores of the concrete were taken from the pavement and examined with an SEM. The concrete was observed to have a highly compact micro-structure with very dense and amorphous C-S-H; this was true even after 3 years of performance under the same conditions (Aitcin and Regourd, 1985). EPMA indicated that the C/S ratios were 1.3 and 0.9, respectively, for 15 and 20% replacement of cement by silica fume, as compared to 1.6 for the ordinary portland cement C-S-H. Clearly, the presence of silica fume modified the composition of C-S-H, more specifically, their calcium content.

Reduction in content of CH

The contribution to strength increase by the pozzolanic reaction mechanism has been viewed differently by Scrivener *et al.* (1984): CH crystals in portland cement paste are sources of weakness due to the fact that cracks can easily propagate through or within these crystals without any significant resistance. The strength increase in the presence of pozzolanic reaction is attributable to the reduction in the content of CH thereby promoting the formation of C-S-H "gel".

Cement paste-aggregate interfacial refinement

The characteristics of the transition zone between the aggregate particles and the cement paste significantly influence the cement-aggregate bond in concrete. Even though the effect of this bond on the performance of concrete has been a subject of controversy (Struble *et al.*, 1980), its significance on the mechanical properties and durability has been established (Mehta, 1983). In normal portland cement concrete, the transition zone is less dense than the bulk paste. Such concrete is also lime-rich, containing a large number of plate-like crystals of CH. The presence of this lime-rich zone is attributable to sand particles acting as sinks for crystallized CH (Regourd, 1985).

The SEM studies by Regourd (1984) demonstrated that the cement aggregate interface was better crystallized and more porous. This interface was more easily subjected to microcracking by tensile stresses caused by applied environmental loads. Consequently, the transition phase between aggregate particles and hydrated cement paste was the weakest link of the concrete system; it had an appreciable influence on the properties of concrete (Mehta, 1983). The pattern of ruptures was described as intergranular (Regourd, 1985). In the presence of silica fume, the interface morphology was different and this was identified as the dominant factor for strength improvement.

Charles-Gilbergues *et al.* (1981) investigated the influence of silica fume on both the thickness of the transition phase and the degree of orientation of the CH crystals in mortar. They reported that the thickness of the transition phase decreased with the addition of silica fume, compared to the reference mortar containing only portland cement. Also, the presence of silica fume reduced the degree of orientation of the CH crystals in the transition phase. On the other hand, both the oriented and continuous films of CH were completely absent at the interface according to Regourd (1984). In addition, no interfacial

cracks were observed and amorphous C-S-H "gel" was seen surrounding the aggregates, thus greatly reducing porosity in this study. In the presence of silica fume, ruptures appeared as granular since bonding was strengthened. Regourd *et al.* (1983) reported an improvement in cement paste-aggregate bonding in blended cements containing only 5% of silica fume. Thus, it is expected that the presence of silica fume in mortar and concrete improves the mechanical properties because of the enhancement in interfacial or bond strength. This strengthening mechanism is not only related to the chemical formation of C-S-H (i.e., pozzolanic reaction) at the interface, but also to the micro-structural modification (i.e., CH orientation, porosity, and transition zone thickness).

Non-pozzolanic Activities

No universal agreement exists among the investigators that the pozzolanic reaction activity is the only source of strength enhancement. Chatterji *et al.* (1982) examined the hydration characteristics of portland cement-silica fume paste and concrete by X-ray diffraction (XRD). The silica fume content varied from 16 to 30% of cement and the w/c ratio ranged from 0.4 to 1.0. The results of XRD indicated that CH was present for at least up to 4 months in the paste, and up to 2 years in the concrete mix. It was noticed that 30% of silica fume could not consume the CH liberated by 70% of portland cement even though the curing temperature was 50°C. The absence of CH from one of the pastes after 5 days of curing was attributed to the lack of water due to a low w/c ratio. As a result, Chatterji *et al.* (1982) have concluded that the strength improvement achieved by adding silica fume to mortar or concrete must be due to the physical nature of the product and not to its pozzolanic activity.

Buil *et al.* (1984) have investigated the hypothesis according to which the principal granular effect of silica fume is the filling of the spaces between the cement grains. The

filling of the spaces between the cement grains might reduce the water/cement ratio and, thus, increase the compressive strength. Nevertheless, these investigators failed to verify the hypothesis, since when silica fume was added to the mortar mixes, the amount of water to be provided to maintain a constant workability requirement had to be increased.

EXPERIMENT

As described in the preceding section, numerous studies were undertaken to investigate the performance of silica fume in concrete. To avoid duplication of past works as well as to reduce the number of variables affecting the performance of concrete, experiments were carried out focusing only on the effects of silica fume content with and without chemical admixtures on the strengths of cement-silica fume mixes and on the characterization of the resultant paste or mortar with SEM, XRD and EDS.

A preliminary investigation indicated that quantitative identification or analysis by SEM, XRD, and EDS of the changes occurring on the surfaces or interior of the surfaces of the paste and mortar as functions of age or time is essentially impossible. This is attributable to the extreme narrowness of the field or area of observation by SEM, XRD and EDS techniques relative to the heterogeneity of the samples. In general, the resolutions of these techniques are limited to the observation of regions on the order of 1 μm . Thus, the SEM micrographs, XRD patterns and EDS spectra were obtained only for the samples at 28 days.

Materials

Materials included Type I portland cement, silica fume, density sand, and chemical admixture for concrete. The silica fume was obtained from Norcem Concrete Products Inc. at Hauppauge, New York; the density sand, a single sized silica sand, from ELE International, Inc./Soiltest Products Division at Lake Bluff, Illinois; and the chemical admixture (DARACEM 100), from W.R. Grace & Co. at Cambridge, Massachusetts.

Equipment

Blender. A heavy-duty, household mixer (KitchenAid Model K45SS Mixer; Figure 3) served as the blender. This mixer comprises a flat beater, a stainless steel bowl, and a variable-speed motor. The rotational speed of the beater ranges from 200 to 1,000 RPM.

Mold. The mold consists of a bottom plate, an upper cover plate with portable rubber gasket, and 10 tubes, each of which is 1 in. in diameter and 2 in. in height (Figure 4). The upper plate tightly covers the mold to prevent loss of moisture during the solidifying and pre-curing stages. The mold can be readily taken apart, cleaned and reassembled.

Capping device. The capping device (Figure 5) adopted is composed of a base and two vertical rods with movable wheels to guide the solidified sample while capping.

Compressive strength tester. The compressive strength was measured by the Tinius Olsen Single Cabinet Hydraulic Digital Super "L" UNIVERSAL Testing Machine with Pressure Transducer Weighing (Figure 6). The major accessories of this tester include a digital load and strain readout, a model MM recorder, an S-type extensometer, and sliding block housings.

X-ray diffractometer (XRD). The XRD analysis was performed with a Siemens D-5000 X-ray diffractometer with $\text{CuK}\alpha$ radiation and 2θ scanning ranging between 10° and 80° .

Scanning electron microscope (SEM). Two scanning electron microscopes were adopted in this study. One is an ETEC-Autoscan scanning electron microscope with a resolution of $20\ \mu\text{m}$, located at the Department of Chemical Engineering, Kansas State

University. It is also equipped with qualitative energy-dispersive X-ray analysis, a backscattered electron detector, and a large (2" x 1") specimen chamber. The other is an HITACHI-S-570 scanning electron microscope (SEM) equipped with a Kevex EDS system containing a germanium detector and diamond window, located at the National Tsing Hua University, Taiwan.

Energy dispersive spectroscope (EDS). The HITACHI-S-570 SEM mentioned above also served the EDS analysis.

Procedure

Mix Design. The samples were prepared according to the mix designs listed in Tables 2 through 7.

Blending. Cement-silica fume paste and mortar were prepared by blending cement, silica fume, water, chemical admixture, and/or sand. The following steps were followed for cement-silica fume paste.

Step 1. Add either cement to silica fume or silica fume to cement depending on which one is abundant, and stir the resultant mixture for approximately 1 minute.

Step 2. Add water and chemical admixture to the resultant mixture from Step 1, and stir it until homogenized.

The following steps were followed for cement-silica fume mortar.

Step 1. Add cement and silica fume to sand, and stir the resultant mixture for approximately 1 minute.

Step 2. Add water and chemical admixture to the resultant mixture from Step 1, and stir it until homogenized.

Casting and curing. The homogenized mixture was poured into molds to obtain cylindrical samples according to the ASTM C192. When solidified, the samples were removed from the molds and placed in a standard moist room until tests were performed on them.

Unconfined compressive strength test. The unconfined compressive strength of solidified samples was determined according to the ASTM standard C39. The solidified samples were tested in triplicate at the ages of 3, 7, 14, 28, and 60 days. Prior to the test, the samples were capped with sulfur mortar according to the ASTM standard C617.

SEM, XRD, and EDS analyses. All the specimens for analyses were prepared and analyzed by specialists according to the standard procedures (see, e.g., Ivey and Neuwirth, 1989).

RESULTS AND DISCUSSION

The results of the present investigation together with some pertinent information are presented in a series of tables, Tables 8 through 12, and a set of diagrams and photographs, Figures 7 through 36. They are detailed below.

In the first series of experiments, samples of cement-silica fume paste were prepared with mixtures of silica fume and portland cement ranging from pure portland cement (0% silica fume) to 90% silica fume in increment of 10%. Addition of water to the cement-silica fume mixture was adjusted to maintain the k-value of the paste's slump at $8 \pm 1/2$ ", measured with the K-Slump Tester, SOILTEST Model CT-385. The mix designs of the pastes are summarized in Table 2. The compressive strengths of the samples were determined in triplicate at the ages of 3, 7, 14, 28, and 60 days. The resultant compressive strengths of the samples are listed in Table 8 and also plotted against the age in Figure 7.

In the second series of experiments, the cement-silica fume paste samples, SW-AA through SW-GG, were prepared with silica fume replacements of 0, 2.5, 5.0, 7.5, 15, and 20%, and their mix designs are shown in Table 3. The resultant compressive strengths of the samples are listed in Table 9 and also depicted in Figure 8. In addition, the SEM micrographs of the paste samples at 28 days are illustrated in Figures 12 and 13.

To investigate the effect of chemical admixture on its performance, the samples of cement-silica fume paste were prepared with silica fume replacements of 0, 2.5, 5.0, 7.5, 15, and 20% and with superplasticizer (Daracem-100) in the third series of experiments. The mix designs of these samples, identified as SW-AA1 through SW-GG1, are summarized in Table 4. The compressive strengths of these samples at various ages are given in Table 10 and Figure 9.

In the fourth series of experiments, the samples of cement-silica fume mortar with up to 25% silica fume replacement were prepared according to mix designs SW-A0 through SW-G0 listed in Table 5. Their compressive strengths are listed in Table 11 and also plotted against the age in Figure 10. The SEM micrographs of the mortar samples at 28 days are illustrated in Figures 14 and 15.

To explore the effect of chemical admixture on the performance of cement-silica fume mortar, the samples were prepared with silica fume replacements of 0, 2.5, 5.0, 7.5, 15, and 20% and a ratio of superplasticizer to cement-silica fume mixture of 0.008:1.00 in the fifth series of experiments. The mix designs of these samples, identified as SW-A1 through SW-G1, are summarized in Table 6. The compressive strengths of these samples at various ages are given in Table 12 and Figure 11.

As mentioned in the literature review section, the improvement in the strengths of cement mixes through the addition of silica fume is mainly attributable to the pozzolanic reaction between the silica fume particles and calcium hydroxide (CH) generated from the hydration of portland cement. Other factors accounting for the improvement include the pore-size refinement and matrix densification, reduction in the content of CH, and cement-aggregate interfacial refinement.

The sixth series of experiments focused on the investigation of mechanisms of the pozzolanic reactions mentioned above by means of the SEM, XRD and EDS techniques. The samples of cement-silica fume paste were prepared according to mix designs S-1 through S-7 given in Table 7. The SEM micrographs of these samples at 28 days are illustrated in Figures 16a through 22c; the XRD patterns, in Figures 23 through 29; and the EDS spectra, in Figures 30 through 36.

Effect of Silica Fume Content on the Performance of Cement-Silica Fume Paste

As shown in Table 8 and Figure 7, the compressive strengths of samples of cement-silica fume paste from the first series of experiments increase with an increase in age; the samples continued to gain in strength up to 60 days. Moreover, the samples with a silica fume replacement of 10% attain the highest strength. This suggests that to obtain the highest strength, the replacement of cement with silica fume is between 0 and 20%; it is approximately 2.5% as can be discerned in Table 9 and Figure 8 containing the results of the second series of experiments in this range. The compressive strength of the cement-silica fume paste decreases with the replacement beyond approximately 2.5%.

It is well known that silica fume by itself does not gel upon mixing with water. It is, therefore, highly plausible that the compressive strength of paste is mainly attributable to the hydration of cement, and silica fume contributes little to the strength. In general, the greater the content of cement, the stronger the paste. Moreover, the inclusion of a relatively small amount of silica fume profoundly accelerates the gain in compressive strength especially at the outset; nevertheless, an ultimate gain in strength after 60 days is small.

Effect of Chemical Admixture on the Performance of Cement-Silica Fume Paste

Results similar to those of the first and second series are obtained in the third series of experiments in which a superplasticizer was added; see Table 10 and Figure 9. Nevertheless, two notable exceptions are observed: (1) water required to maintain the desirable slump is reduced, thereby resulting generally in moderate increases in the compressive strengths compared to those without the addition of the superplasticizer, and (2) the gain in the strength is highest at a silica fume replacement of 5% instead of 2.5%.

Effect of Silica Fume Content on the Performance of Cement-Silica Fume Mortar

In the fourth series of experiments, the ratio of density sand to the mixture of cement and silica fume was 4:1, and that of water to the same mixture was 0.75:1.00; see Table 5. As expected, the compressive strengths of mortar samples increase with an increase in age; the samples continue to gain their strengths up to 60 days; see Table 11 and Figure 10. Moreover, the samples with a silica fume replacement of 7.5% attain the highest strength. Nevertheless, the strengths of mortar samples are substantially less than those of paste samples of the same ages; the strengths range from 1,250 psi to 2,750 psi for the former, and from 5,000 psi to 8,500 psi for the latter. Furthermore, the compressive strength of the cement-silica fume mortar decrease with the replacement beyond approximately 7.5% instead of 2.5% for the cement-silica fume paste. It is well known that the strength of mortar depends on the type and shape of sand employed, and that the hydrated cement functions as a "glue" to link the particles of the sand. The higher the quality of sand, the higher the amount of cement added, and the lower the water/cement ratio, the greater the strength.

Effect of Chemical Admixture on the Performance of Cement-Silica Fume Mortar

For comparison, the ratio of density sand to the mixture of cement and silica fume in the fifth series of experiments was maintained at 4:1 (the same as in the fourth series of experiments). Results similar to those of the fourth series are obtained except that the compressive strengths are substantially less for those with superplasticizer than those without; see Table 12 and Figure 11. Note that the ratio of water to the mixture of cement and silica fume is reduced from 0.75:1.00 to 0.672:1.00 to maintain a desirable slump. This indicates that the reduction of water by adding superplasticizer in the mortar containing certain amounts of silica fume does not increase the compressive strengths of

the samples of cement-silica fume mortar as anticipated.

SEM Analysis

The SEM micrographs of samples of cement-silica fume paste with various compositions at 28 days are presented in Figures 12 and 13. These photos were taken at KSU at a magnification of 100X for the former and 3,000X for the latter. While scanning the surfaces of Samples SW-AA through SW-GG at magnifications of 100X and 3,000X, no significant differences in the appearance are observed; see Figures 12 and 13.

The SEM micrographs of samples of cement-silica fume mortar with various compositions at 28 days are illustrated in Figures 14 and 15. These photos were also taken at KSU at a magnification of 100X for the former and 3,000X for the latter. Gel-like (amorphous) calcium silica hydrate is observed covering the clinker and the sand grains in Samples SW-A0 through SW-G0. Needle-like ettringite and crystalline-like calcium hydroxide are also observed in these samples; see Figures 14 and 15.

The SEM micrographs of samples of cement-silica fume paste at a magnification of 10,000X were taken at the National Tsing Hua University, Taiwan. The samples were prepared according to the mix designs listed in Table 7. Three SEM micrographs were taken at 28 days for each of the samples. They are given in Figures 16a through 22c. To obtain additional information on the structures of the surfaces of these samples so as to facilitate interpretation, their XRD patterns and EDS spectra were also taken, as will be discussed later.

Figures 16a through 16c are the typical SEM micrographs of the hydrated cement. Gel-like (amorphous) calcium silica hydrate is observed covering the clinker grains in Sample S-1. Needle-like ettringite and granular and smaller calcium hydroxide crystals are

also observed in the sample. Similar observations can be made in Samples S-2 through S-6. Unreacted silica-fume spheres exist in these samples; see Figures 17a through 21c. Figures 22a through 22c are the SEM micrographs of the silica fume sample. Note that Figure 22c reveals some impurities.

SEM is effective in providing information on the major characteristics of phases on the surfaces of solid materials. The resolution of SEM is limited, however, to the observation of regions on the order of 1 μm in the samples. Since the samples investigated are both heterogeneous and nonhomogeneous, SEM cannot describe the system completely.

XRD Analysis

The XRD analyses of samples of cement-silica fume paste with various compositions at 28 days were carried out at the National Tsing Hua University, Taiwan and are presented in Figures 23 through 29. The major compounds identified in the samples of cement-silica fume paste include SiO_2 , $\text{Ca}(\text{OH})_2$, $2\text{CaO}\cdot\text{Fe}_2\text{O}_3$, $2\text{CaO}\cdot\text{SiO}_2$, $2\text{CaO}\cdot\text{SiO}_2\cdot\text{H}_2\text{O}$, $3\text{CaO}\cdot\text{Al}_2\text{O}_3\cdot 3\text{CaSO}_4\cdot 31\text{H}_2\text{O}$, $4\text{CaO}\cdot\text{Al}_2\text{O}_3\cdot 13\text{H}_2\text{O}$, and $6\text{CaO}\cdot 4\text{SiO}_2\cdot 3\text{H}_2\text{O}$, or in the parlance of cement chemistry S, CH, C_2F , C_2S , C_2SH , Etc., C_4AH_{13} , and $\text{C}_6\text{S}_4\text{H}_3$, respectively. The appearance of CH in Samples S-1 through S-6 indicates that hydration of cement occurs in these samples. Compound SiO_2 is the only component identified in Sample S-7; see Figure 29. This indicates that no hydration takes place in this sample.

XRD is effective for studying the changes in crystallinity and the appearance or disappearance of crystalline phases on the surfaces of solid materials. The effectiveness of XRD is limited in the sense that it reveals only the crystalline components. Since some of

the materials in the samples are expected to be amorphous, XRD is incapable of yielding complete information on the system.

EDS Analysis

The EDS spectra of Samples S-1 through S-7 were taken at the National Tsing Hua University, Taiwan with an HITACHI-S-570 SEM equipped with a kevox EDS system; they are presented in Figures 30 through 36. The elements identified in these samples include Al, Ca, Fe, K, Mg, S, and Si. The weight and atomic percentages of these elements in each sample are also shown in these figures. As expected, the weight ratio of Ca/Si decreases with an increase in the content of silica fume in the samples; it is 12.60 for Sample S-1, 8.18 for Sample S-3, and 4.01 for Sample S-6. Note that Sample S-1 is hydrated cement without silica fume, whereas Samples S-3 and S-6 are hydrated paste with a replacement of cement with silica fume of 20 wt% and 50 wt%, respectively. Nevertheless, no correlation can be discerned between the Ca/Si ratio and the compressive strength of the samples.

Note that EDS identifies only elemental compositions of the surfaces of solid materials. It cannot differentiate, therefore, the types of compounds formed from the elements.

CONCLUDING REMARKS

The significant conclusions reached in the present investigation are as follows:

1. For cement-silica fume paste, the samples with a silica fume replacement of around 2.5 wt% and without superplasticizer gained the highest strength at 28 days. With the addition of the superplasticizer, the samples required less water to maintain a desirable slump, thereby resulting generally in moderate increases in the compressive strength compared to those without, and the gain in the strength was highest at a silica fume replacement of 5.0 wt% instead of 2.5 wt%.

2. For cement-silica fume mortar, the samples with a silica fume replacement of approximately 7.5 wt% and with or without superplasticizer gained the highest strength at 28 days. The reduction of water by adding superplasticizer in the mortar containing silica fume did not increase the compressive strengths of the samples of cement-silica fume mortar as anticipated.

3. No significant differences in the appearance were observed while scanning the surfaces of the samples of cement-silica fume paste at magnifications of 100X and 3,000X. Gel-like calcium silica hydrate was, however, observed covering the clinker and the sand grains in the cement-silica fume mortar. Needle-like ettringite and crystalline calcium hydroxide were also observed in these samples.

4. The major compounds identified in the samples of cement-silica fume paste by the XRD included SiO_2 , Ca(OH)_2 , $2\text{CaO.Fe}_2\text{O}_3$, 2CaO.SiO_2 , $2\text{CaO.SiO}_2.\text{H}_2\text{O}$, $3\text{CaO.Al}_2\text{O}_3.3\text{CaSO}_4.31\text{H}_2\text{O}$, $4\text{CaO.Al}_2\text{O}_3.13\text{H}_2\text{O}$, and $6\text{CaO}.4\text{SiO}_2.3\text{H}_2\text{O}$. Compound SiO_2 was the only component identified in the sample of pure silica fume, thereby indicating that no hydration took place in this sample.

5. The elements identified in the samples of cement-silica fume paste by the EDS included Al, Ca, Fe, K, Mg, S, and Si. No correlation, however, could be discerned between the Ca/Si ratio and the compressive strength of the samples.

On the basis of the results obtained, the optimal mix designs for the cement paste and mortar in terms of their compressive strengths appear to be as follows:

a. For cement-silica fume paste, the optimal replacement of cement with silica fume is approximately 5.0 wt% with the addition of superplasticizer and 2.5 wt% without.

b. For cement-silica fume mortar, the optimal replacement of cement with silica fume is approximately 7.5 wt% both with and without the addition of superplasticizer.

Naturally, extensive investigation is required for further confirmation of the optimal mix designs proposed herein.

REFERENCES

- Aitcin, P. C. and M. Regourd, "The Use of Condensed Silica Fume to Control Alkali-Silica Reaction: A Field Case Study," *Cement and Concrete Research*, **15**, pp. 711-719 (1985).
- Aitcin, P. C. and D. Vezina, "Resistance to Freezing and Thawing of Silica Fume Concrete," *Cement, Concrete, and Aggregates, CCAGDP*, Vol. 6, No. 1, pp. 38-42, Summer 1984.
- Bache, H.H., "Densified Cement/Ultrafine Particle-Based Materials," Second International Conference on Superplasticizers in Concrete, Ottawa, Canada 1981.
- Berke, N. S., D. W. Pfeifer, and T. G. Weil, "Protection Against Chloride-Induced Corrosion," *Concrete International*, pp. 45-54, December 1988.
- Buck, A. D. and J. P. Burkes, "Characterization and Reactivity of Silica Fume," Proceedings of the 3rd International Conference on Cement Microscopy, pp. 279-285, Houston, Texas, March 1981.
- Buil, M., A. M. Paillere, and B. Roussel, "High-Strength Mortars Containing Condensed Silica Fume," *Cement and Concrete Research*, **14**, pp. 693-704 (1984).
- Charles-Gibergues, A., J. Grandet, and J. P. Ollivier, Materials Research Society, Symposium on Fly Ash Incorporation in Cement and Concrete, Boston, Massachusetts, November 1981.
- Chatterji, S., N. Thaulow, and P. Christensen, "Pozzolanic Activity of By-Product Silica Fume from Ferro-Silicon Production," *Cement and Concrete Research*, **12**, pp. 781-784 (1982).
- Cheng, Y. H. and R. F. Feldman, "Hydration Reactions in Portland Cement-Silica Fume Blends," *Cement and Concrete Research*, **15**, pp. 585-592 (1985).
- Cohen, M. D., J. Olek, and B. Mather, "Silica Fume Improves Expansive-Cement Concrete," *Concrete International*, pp. 31-37, March 1991.
- Cohen, M. D. and J. Olek, "Silica Fume in PCC: The Effects of Form on Engineering Performance," *Concrete International*, pp. 43-77, November 1989.
- Detwiler, G., "High-Strength Silica Fume Concrete: Chicago Style," *Concrete International*, pp. 43-77, October 1992.

- Durning, T. A. and M. C. Hicks, "Using Microsilica to Increase Concrete's Resistance to Aggressive Chemicals," *Concrete International*, pp. 42-48, March 1991.
- Grutzeck, M. W., D. M. Roy, and D. Wolfe-Confer, "Mechanism of Hydration of Portland Cement Containing Ferro-Silicon Dust," *Proceedings of the 4th International Conference on Cement Microscopy*, Ed. G. R. Gouda, pp. 193-202, Las Vegas, Nevada 1982.
- Grutzeck, M. W., S. Atkinson, and D. M. Roy, "Mechanism of Hydration of Condensed Silica Fume in Hydroxide Solution," *Publication of the American Concrete Institute*, SP 79, pp. 643-665 (1983).
- Holland, T. C. and R. A. Gutschow, "Erosion Resistance with Silica-Fume Concrete," *Concrete International*, pp. 32-40, March 1987.
- Ivey, D. G. and M. Neuwirth, "A Technique for Preparing TEM Specimens from Cementitious Materials," *Cement and Concrete Research*, **19**, pp. 642-648 (1989).
- Jahr, J., "Possible Health Hazards from Different Types of Amorphous Silicas - Suggested Threshold Limit Values," *Institute of Occupational Health*, Oslo 1980.
- Kurbus, B., F. Bakula, and R. Gabrovser, "Reactivity of SiO₂ Fume from Ferro-Silicon Production with Ca(OH)₂ under Hydrothermal Conditions," *Cement and Concrete Research*, **15**, pp. 134-140 (1985).
- Lessard, M., S. L. Sarkar, D. W. Ksinsik, and P. C. Aitcin, "Long-Term Behavior of Silica Fume Concrete," *Concrete International*, pp. 25-30, April 1992.
- Luther, M. D., "Silica Fume (Microsilica) Concrete in Bridges," *Concrete International*, pp. 29-33, April 1993.
- Malhotra, V. M. and G. G. Carette, "Silica Fume Concrete: Properties, Applications, and Limitations," *Concrete International*, pp. 40-46, May 1983.
- Mehta, P.K. and O. E. Gjorv, "Properties of Portland Cement Concrete Containing Fly Ash and Condensed Silica Fume," *Cement and Concrete Research*, **12**, pp. 587-595 (1982).
- Mehta, P. K., "Studies of Blended Portland Cement Containing Santorin Earth," *Cement and Concrete Research*, **11**, pp. 507-518 (1981).
- Mehta, P. K., "Pozzolanic and Cementitious By-products as Mineral Admixtures for Concrete: A Critical Review," *Publication of the American Concrete Institute*, SP 79, pp. 1-45 (1983).

- Nelson, J. A. and J. F. Young, "Additions of Colloidal Silicas and Silicates to Portland Cement Pastes," *Cement and Concrete Research*, **7**, pp. 277-282 (1977).
- Oberholster, R.E. and W.B. Westra, "The Effectiveness of Mineral Admixtures in Reducing Expansion due to Alkali-Aggregate Reaction with Malmesbury Group Aggregates," *Proceedings of the 5th International Conference on Alkali-Aggregate Reactions in Concrete* (Cape Town, Apr. 1981), National Building Research Institute, Pretoria, 1981 Paper No. S 242/31, 10 pp.
- Regourd, M., "Microstructure of High Strength Cement Paste Systems," *Materials Research Society, Very High Strength Cement-Based Materials*, Ed., J. F. Young, **42**, pp. 3-17 (1985).
- Regourd, M., B. Murtureux, and H. Hornain, "Use of Condensed Silica Fume as Filler in Blended Cements," *Publication of the American Concrete Institute, SP 79*, pp. 847-865 (1983).
- Regourd, M., B. Murtureux, P. C. Aitcin, and P. Pinsonheault, "Microstructure of Concrete Containing Silica Fume," *Proceedings of the 4th International Conference on Cement Microscopy*, Ed. G. R. Gouda, pp. 249-260, Las Vegas, Nevada 1982.
- Scriverer, K. L., K. D. Boldie, Y. Halse, and P. C. Pratt, "Characterization of Microstructure as a Systematic Approach to High Strength Cements," *Materials Research Society, Very High Strength Cement-Based Materials*, Ed., J. F. Young, **42**, pp. 39-43 (1985).
- Sellevoid, E. J., D. H. Badger, E. K. Jensen, and T. Knudsen, "Silica Fume Pastes: Hydration and Structure," *Proceedings of Nordisk Miniseminar on Silica in Concrete*, Troodbeim, December 1981.
- Struble, L., J. Skalny, and S. Mindess, "A Review of the Cement-Aggregate Bond," *Cement and Concrete Research*, **10**, pp. 277-286 (1980).
- Traetteberg, A., "Silica Fume as a Pozzolanic Material," *Cemento*, **75**, pp. 369-375 (1978).
- Wolsiefer, J., "Ultra High Strength Field Placeable Concrete in the Range 10,000 to 18,000 psi," paper presented at the 1982 ACI Annual Convention, Atlanta.

Table 1. Chemical Composition of Silica Fumes from Silicon Furnace in Norway and North America

Constituent	Norway* %	North America** %
SiO ₂	90.0 - 96.0	98.0
Al ₂ O ₃	0.5 - 3.0	0.3
Fe ₂ O ₃	0.2 - 0.8	0.8
MgO	0.5 - 1.5	0.2
CaO	0.1 - 0.5	0.2
Na ₂ O	0.2 - 0.7	0.2
K ₂ O	0.4 - 1.0	0.5
C	0.5 - 1.4	2.5
S	0.1 - 0.4	0.1
LOI	0.7 - 2.5	2.8

* From the brochure of Elkem Silica - Spigerverket A/S, Norway.

** From a plant in Eastern Canada.

Table 2. Mix Designs for Preparing Samples SW-A through SW-J of Cement-Silica Fume Paste

Material	Mix Design										
	SW-A	SW-B	SW-C	SW-D	SW-E	SW-F	SW-G	SW-H	SW-I	SW-J	
											Weight (grams)
1. Portland cement	100.0	90.0	80.0	70.0	60.0	50.0	40.0	30.0	20.0	10.0	
2. Silica fume	0.0	10.0	20.0	30.0	40.0	50.0	60.0	70.0	80.0	90.0	
3. Water	30.0	30.0	30.0	31.0	32.5	34.0	37.50	40.0	43.0	46.0	
Total	130.0	130.0	130.0	131.0	132.5	134.0	137.5	140.0	143.0	146.0	

Table 3. Mix Designs for Preparing Samples SW-AA through SW-GG of Cement-Silica Fume Paste

Material	Mix Design										
	SW-AA	SW-BB	SW-CC	SW-DD	SW-EE	SW-FF	SW-GG				
											Weight (grams)
1. Portland cement	100.00	97.50	95.00	92.50	90.00	85.00	80.00				
2. Silica fume	0.00	2.50	5.00	7.50	10.00	15.00	20.00				
3. Water	30.00	30.00	30.00	30.00	30.00	30.00	30.00				
Total	130.00	130.00	130.00	130.00	130.00	130.00	130.00				

Table 4. Mix Designs for Preparing Samples SW-AA1 through SW-GG1 of Cement-Silica Fume Paste

Material	Mix Design										
	SW-AA1	SW-BB1	SW-CC1	SW-DD1	SW-EE1	SW-FF1	SW-GG1				
	Weight (grams)										
1. Portland cement	100.00	97.50	95.00	92.50	90.00	85.00	80.00				
2. Silica fume	0.00	2.50	5.00	7.50	10.00	15.00	20.00				
3. Water	24.50	24.50	25.50	26.00	27.00	28.00	29.00				
4. Daracem 100	0.53	0.53	0.53	0.53	0.53	0.53	0.53				
Total	125.03	125.03	126.03	126.53	127.53	128.53	129.53				

Table 5. Mix Designs for Preparing Samples SW-A0 through SW-G0 of Cement-Silica Fume Mortar

Material	Mix Design										
	SW-A0	SW-B0	SW-C0	SW-D0	SW-E0	SW-F0	SW-G0				
	Weight (grams)										
1. Density sand	100.00	100.00	100.00	100.00	100.00	100.00	100.00				
2. Portland cement	25.00	24.37	23.75	23.12	22.50	21.25	20.00				
3. Silica fume	0.00	0.63	1.25	1.87	2.50	3.75	5.00				
4. Water	17.50	17.50	17.50	17.50	17.50	17.50	17.50				
Total	142.50	142.50	142.50	142.50	142.50	142.50	142.50				

Table 6. Mix Designs for Preparing Samples SW-A1 through SW-G1 of Cement-Silica Fume Mortar

Material	Mix Design						
	SW-A1	SW-B1	SW-C1	SW-D1	SW-E1	SW-F1	SW-G1
	Weight (grams)						
1. Density sand	100.00	100.00	100.00	100.00	100.00	100.00	100.00
2. Portland cement	25.00	24.37	23.75	23.12	22.50	21.25	20.00
3. Silica fume	0.00	0.63	1.25	1.87	2.50	3.75	5.00
4. Water	16.80	16.80	16.80	16.80	16.80	16.80	16.80
5. Daracem 100	0.20	0.20	0.20	0.20	0.20	0.20	0.20
Total	142.00	142.00	142.00	142.00	142.00	142.00	142.00

Table 7. Mix Designs for Preparing Samples S-1 through S-7 of Cement-Silica Fume Paste

Material	Mix Design						
	S-1	S-2	S-3	S-4	S-5	S-6	S-7
	Weight (grams)						
1. Portland cement	100.00	90.00	80.00	70.00	60.00	50.00	0.00
2. Silica fume	0.00	10.00	20.00	30.00	40.00	55.00	100.00
3. Water	30.00	30.00	30.00	31.00	32.50	34.00	48.00
Total	130.00	130.00	130.00	131.00	132.50	134.00	148.00

Table 8a. Compressive Strengths of Samples of Cement-Silica Fume Paste:
SW-A through SW-E

Age	Mix Design				
	SW-A	SW-B	SW-C	SW-D	SW-E
	Compressive Strength (psi)				
3 days	6,130.0	6,027.0	4,773.0	4,285.0	3,068.0
7 days	6,897.0	7,130.0	5,783.0	4,580.0	3,633.0
14 days	7,737.0	8,240.0	6,485.0	5,184.0	3,429.0
28 days	7,060.0	7,363.0	6,093.0	4,847.0	3,713.0
60 days	8,160.0	8,360.0	6,813.0	5,860.0	3,970.0

Table 8b. Compressive Strengths of Samples of Cement-Silica Fume Paste:
SW-F through SW-J

Age	Mix Design				
	SW-F	SW-G	SW-H	SW-I	SW-J
	Compressive Strength (psi)				
3 days	1,961.0	1,383.0	701.0	524.0	172.0
7 days	2,163.0	1,534.0	1,267.0	708.0	233.0
14 days	2,542.0	1,661.0	1,469.0	728.0	285.0
28 days	2,671.0	2,161.0	1,870.0	770.0	365.0
60 days	3,170.0	2,833.0	1,929.0	932.0	398.0

Table 9. Compressive Strengths of Samples of Cement-Silica Fume Paste:
SW-AA through SW-GG

Age	Mix Design						
	SW-AA	SW-BB	SW-CC	SW-DD	SW-EE	SW-FF	SW-GG
	Compressive Strength (psi)						
3 days	5,830.0	6,053.0	6,367.0	6,273.0	6,027.0	5,287.0	4,889.0
7 days	6,150.0	7,290.0	6,670.0	6,480.0	6,640.0	6,250.0	5,560.0
14 days	6,417.0	7,773.0	6,710.0	6,940.0	7,183.0	6,563.0	6,107.0
28 days	7,260.0	8,010.0	7,067.0	7,443.0	7,703.0	6,867.0	6,610.0
60 days	8,423.0	8,520.0	7,930.0	8,160.0	7,563.0	7,270.0	7,120.0

Table 10. Compressive Strengths of Samples of Cement-Silica Fume Paste:
SW-AA1 through SW-GG1

Age	Mix Design						
	SW-AA1	SW-BB1	SW-CC1	SW-DD1	SW-EE1	SW-FF1	SW-GG1
	Compressive Strength (psi)						
3 days	5,593.0	5,930.0	6,153.0	6,437.0	5,563.0	5,077.0	4,810.0
7 days	6,947.0	6,445.0	6,667.0	6,567.0	6,417.0	5,580.0	4,915.0
14 days	7,620.0	7,387.0	8,605.0	7,300.0	7,000.0	6,803.0	5,950.0
28 days	7,483.0	8,053.0	8,830.0	8,545.0	7,320.0	7,040.0	6,117.0
60 days	7,740.0	8,935.0	9,170.0	8,735.0	7,570.0	7,710.0	6,110.0

Table 11. Compressive Strengths of Samples of Cement-Silica Fume Mortar:
SW-A0 through SW-G0

Age	Mix Design						
	SW-A0	SW-B0	SW-C0	SW-D0	SW-E0	SW-F0	SW-G0
	Compressive Strength (psi)						
3 days	1,295.0	1,267.0	1,308.0	1,627.0	1,377.0	1,324.0	1,460.0
7 days	1,626.0	1,503.0	1,635.0	1,848.0	1,801.0	1,543.0	1,639.0
14 days	1,765.0	1,710.0	1,712.0	1,872.0	1,814.0	1,842.0	1,846.0
28 days	2,278.0	2,184.0	2,336.0	2,520.0	2,335.0	2,231.0	2,183.0
60 days	2,458.0	2,636.0	2,698.0	2,796.0	2,721.0	2,314.0	2,373.0

Table 12. Compressive Strengths of Samples of Cement-Silica Fume Mortar:
SW-A1 through SW-G1

Age	Mix Design						
	SW-A1	SW-B1	SW-C1	SW-D1	SW-E1	SW-F1	SW-G1
	Compressive Strength (psi)						
3 days	952.0	1,214.0	1,170.0	1,030.0	1,170.0	1,126.0	977.0
7 days	1,288.0	1,397.0	1,433.0	1,441.0	1,457.0	1,338.0	1,258.0
14 days	1,567.0	1,552.0	1,787.0	1,732.0	1,812.0	1,504.0	1,302.0
28 days	1,830.0	1,849.0	1,863.0	2,079.0	2,079.0	1,746.0	1,767.0
60 days	2,141.0	2,034.0	2,376.0	2,222.0	2,135.0	2,082.0	1,991.0

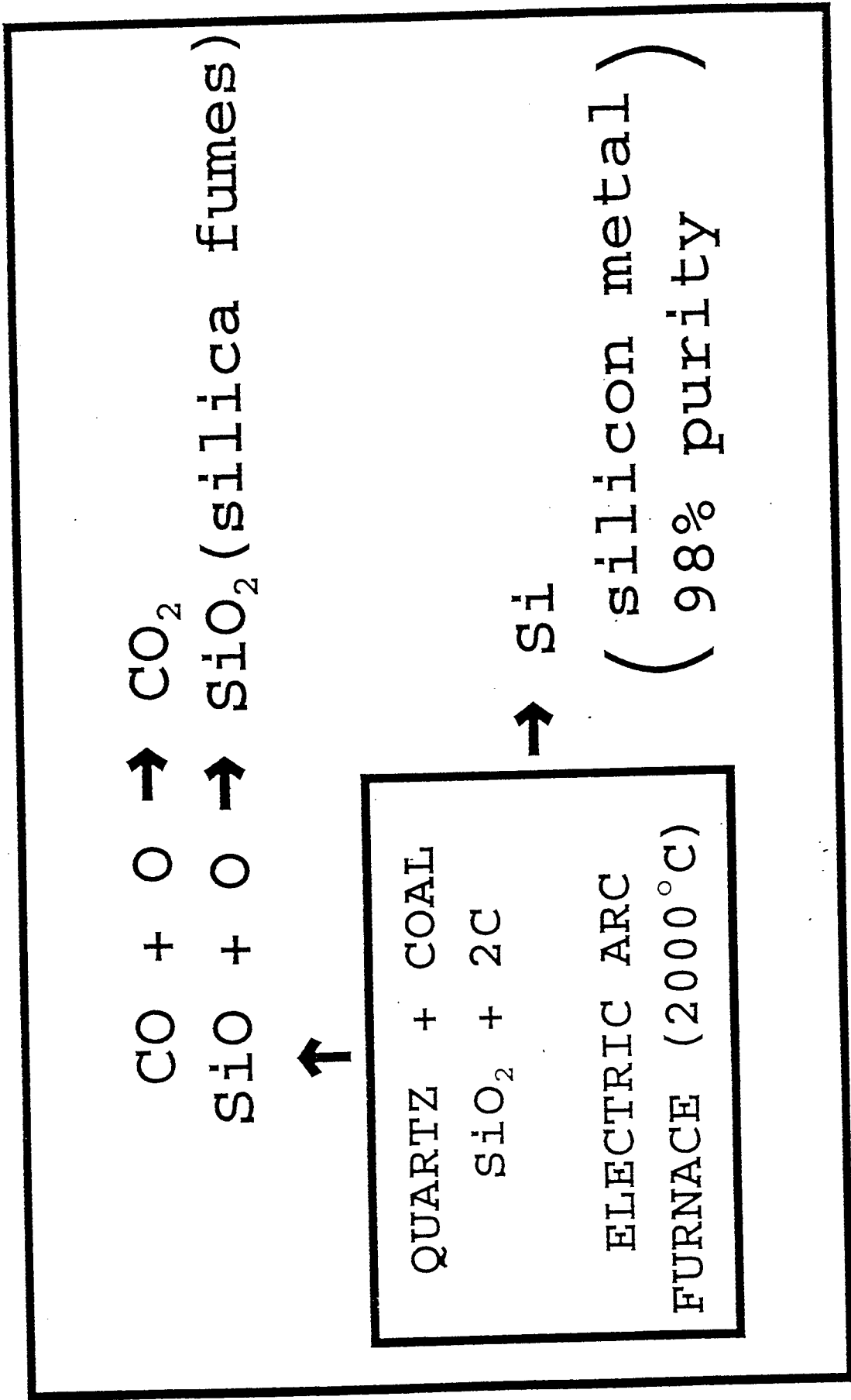


Figure 1. Generation of silica fume as a by-product in the production of silicon metal.

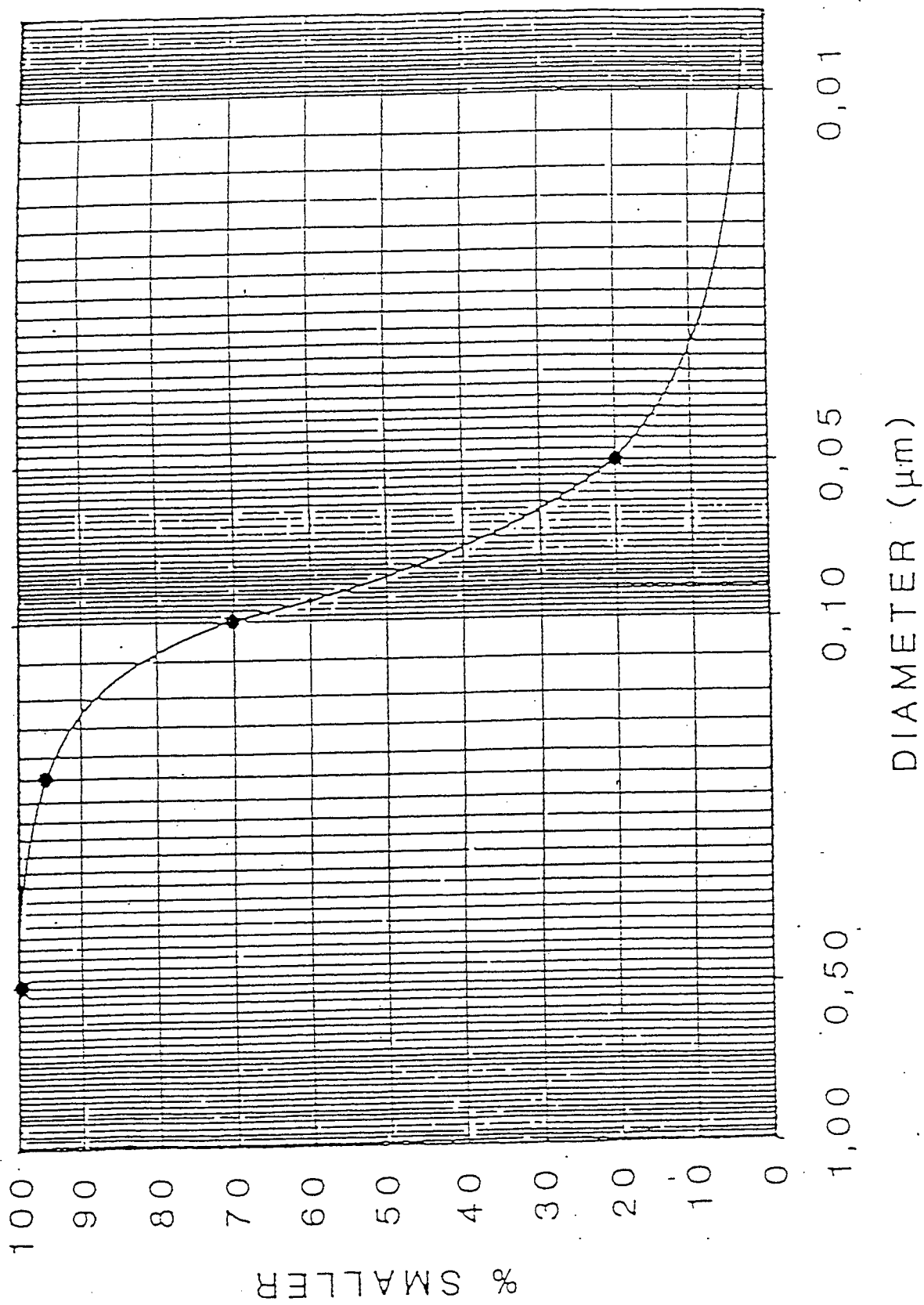


Figure 2. Particle-size distribution of silica fume from a Canadian plant.



Figure 3. Blender.

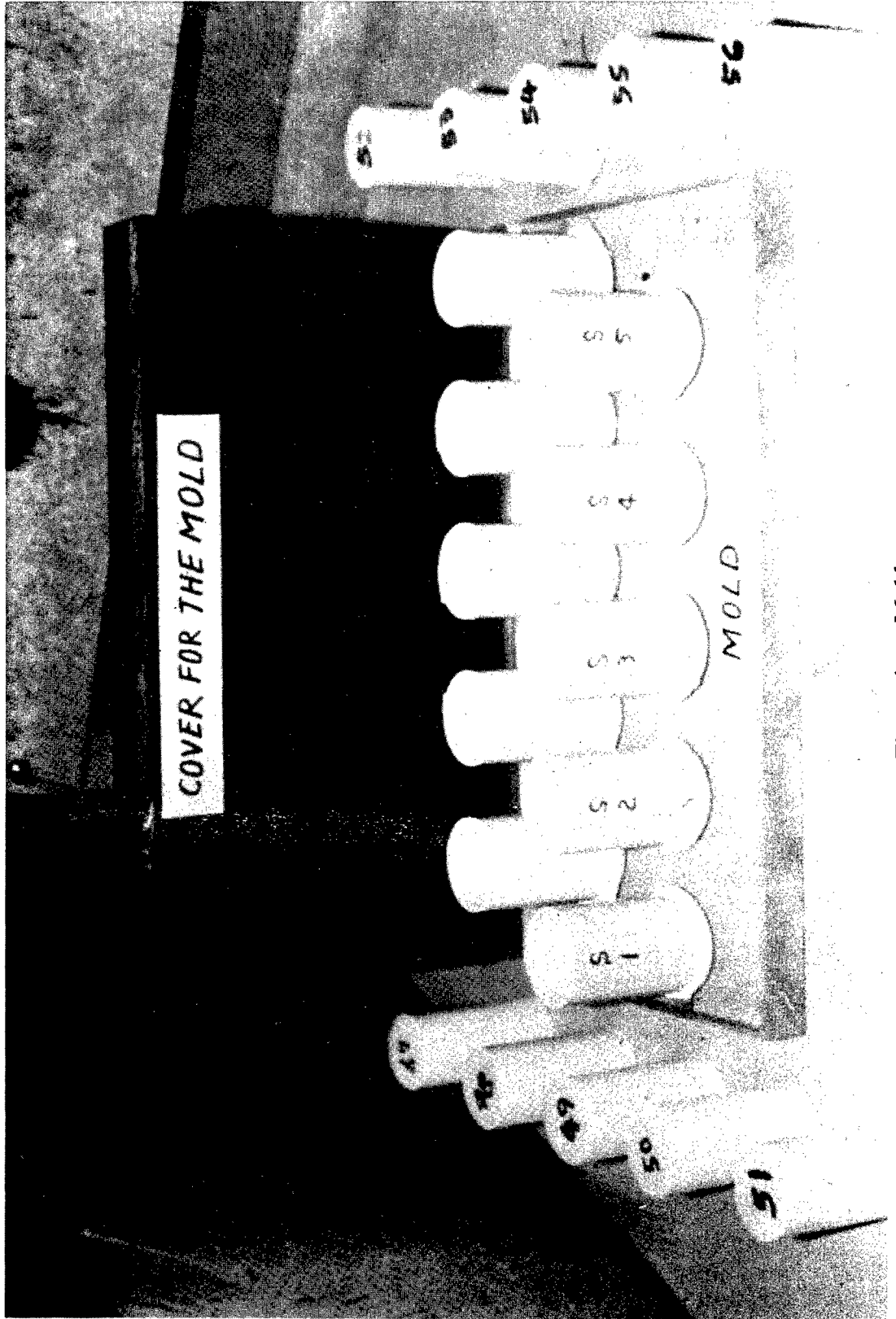


Figure 4. Mold.

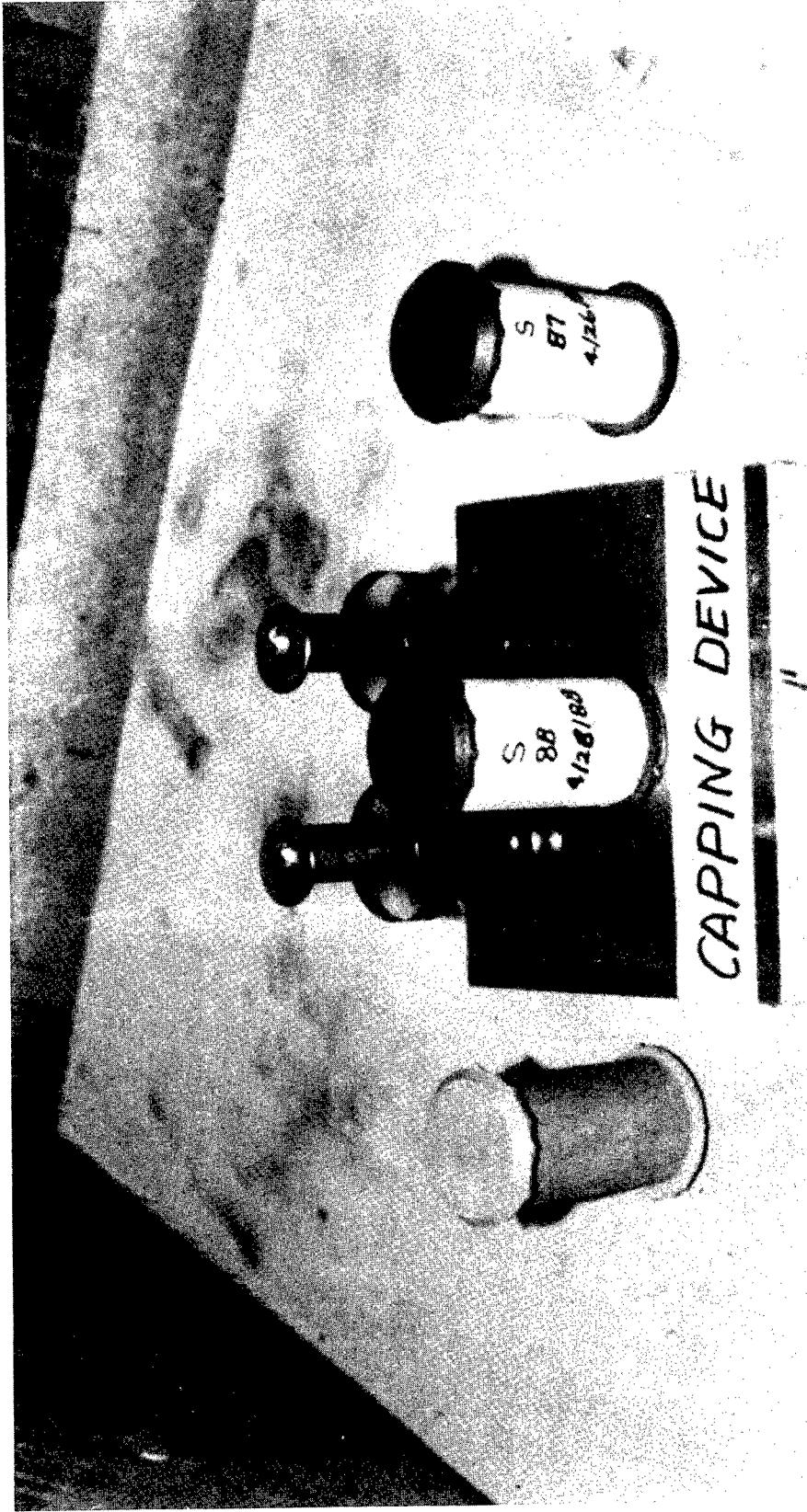


Figure 5.™ Miniature capping device.

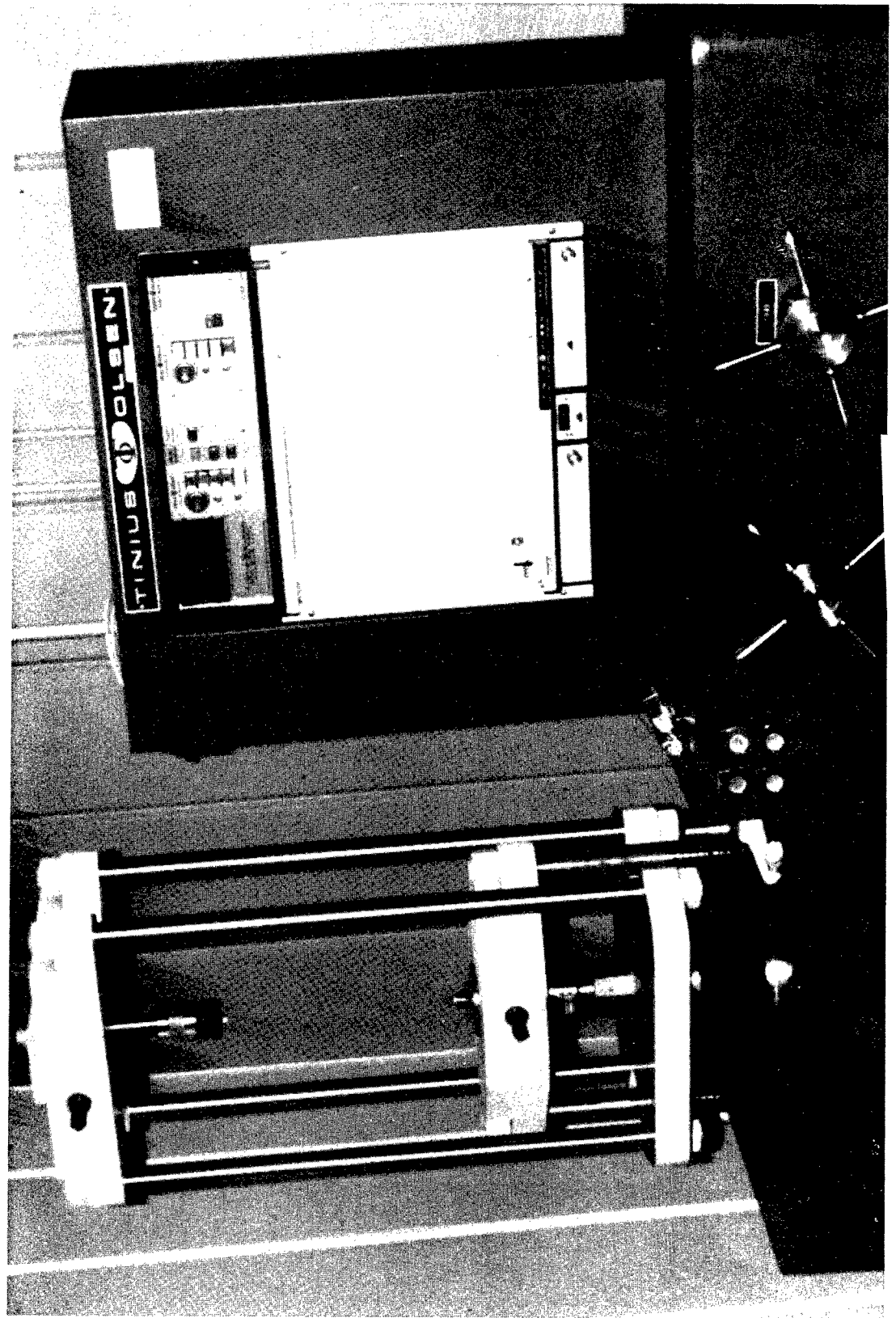


Figure 6. Compressive strength tester.

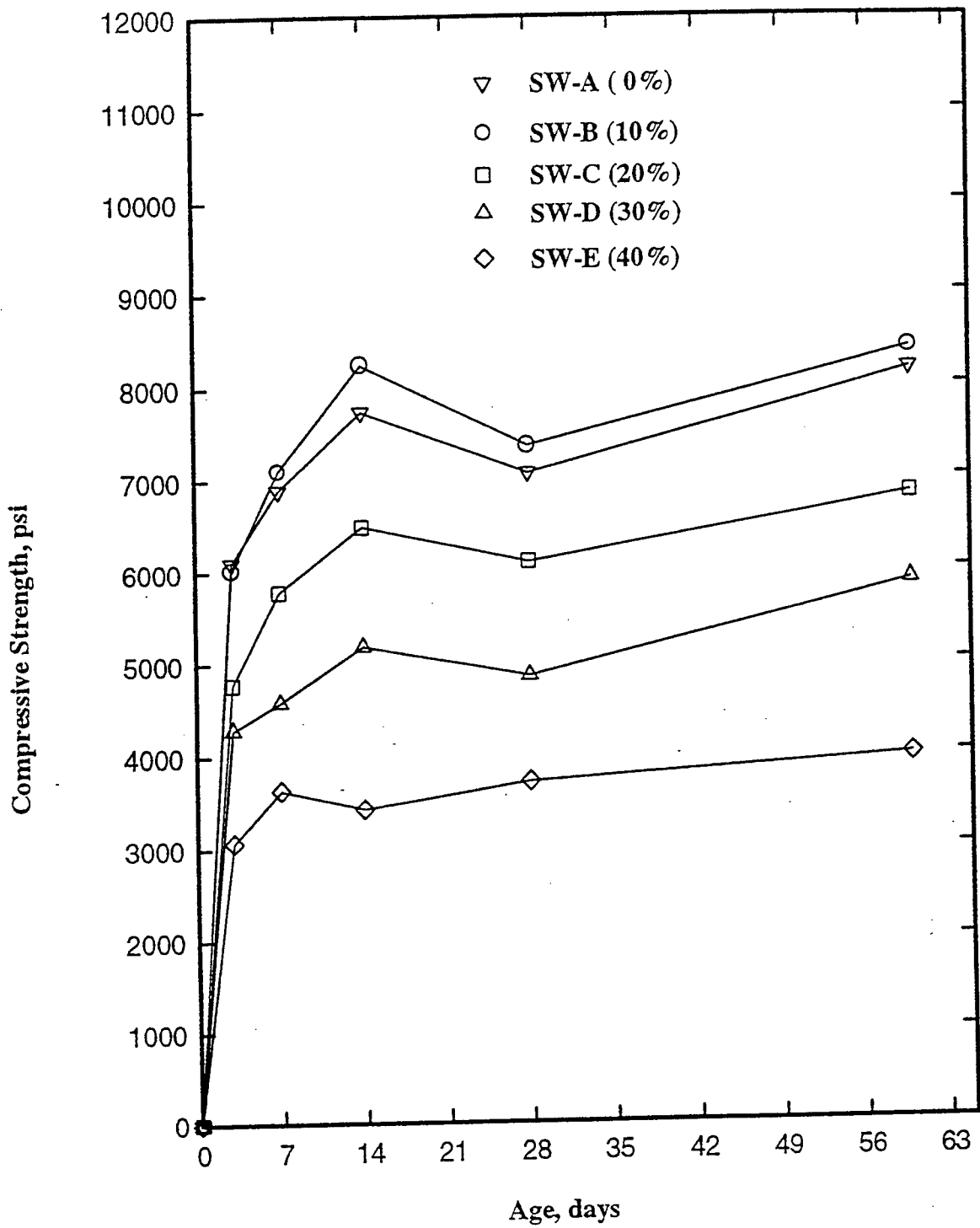


Figure 7a. Compressive strengths of samples of cement-silica fume paste: SW-A through SW-E.

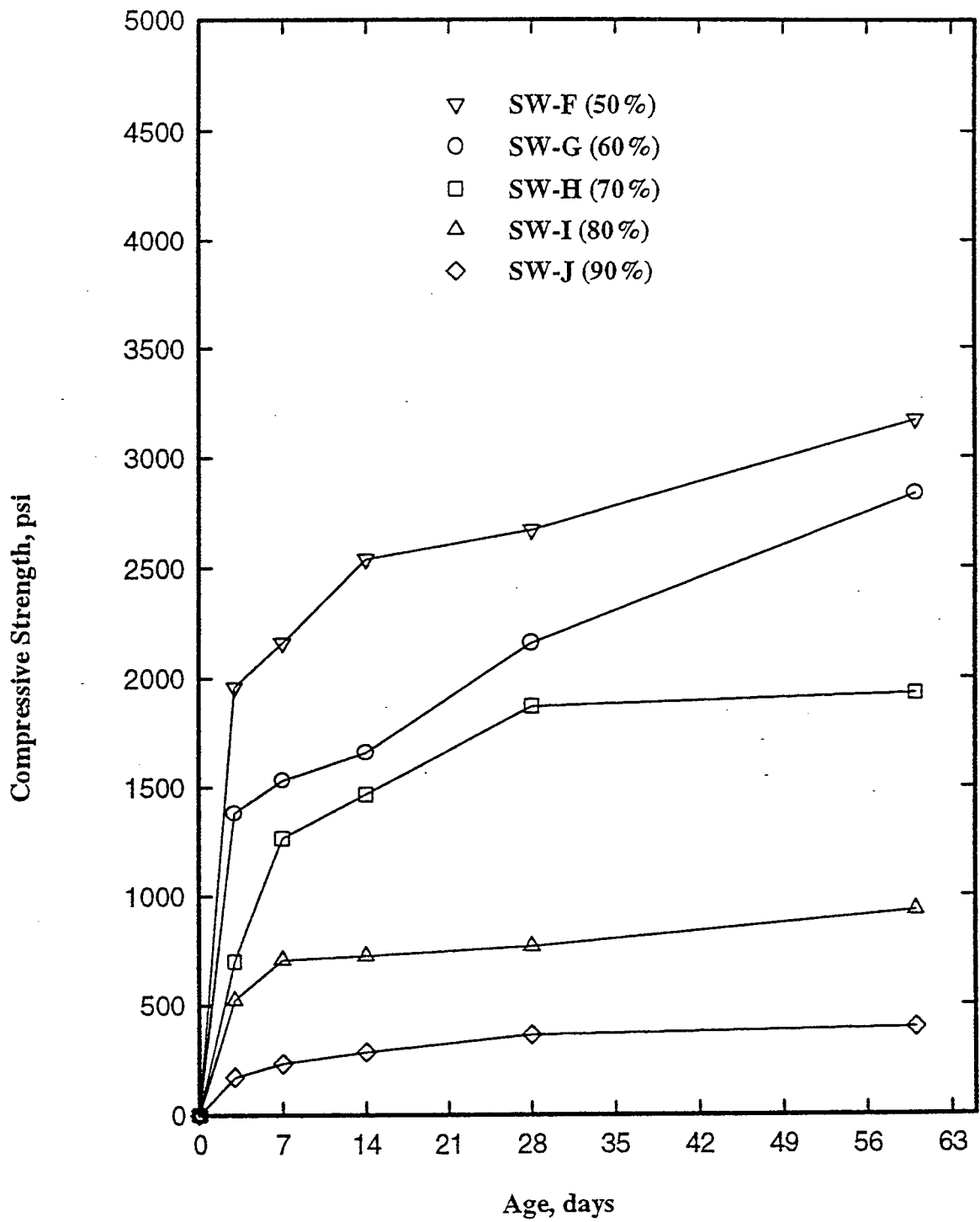


Figure 7b. Compressive strengths of samples of cement-silica fume paste: SW-F through SW-J.

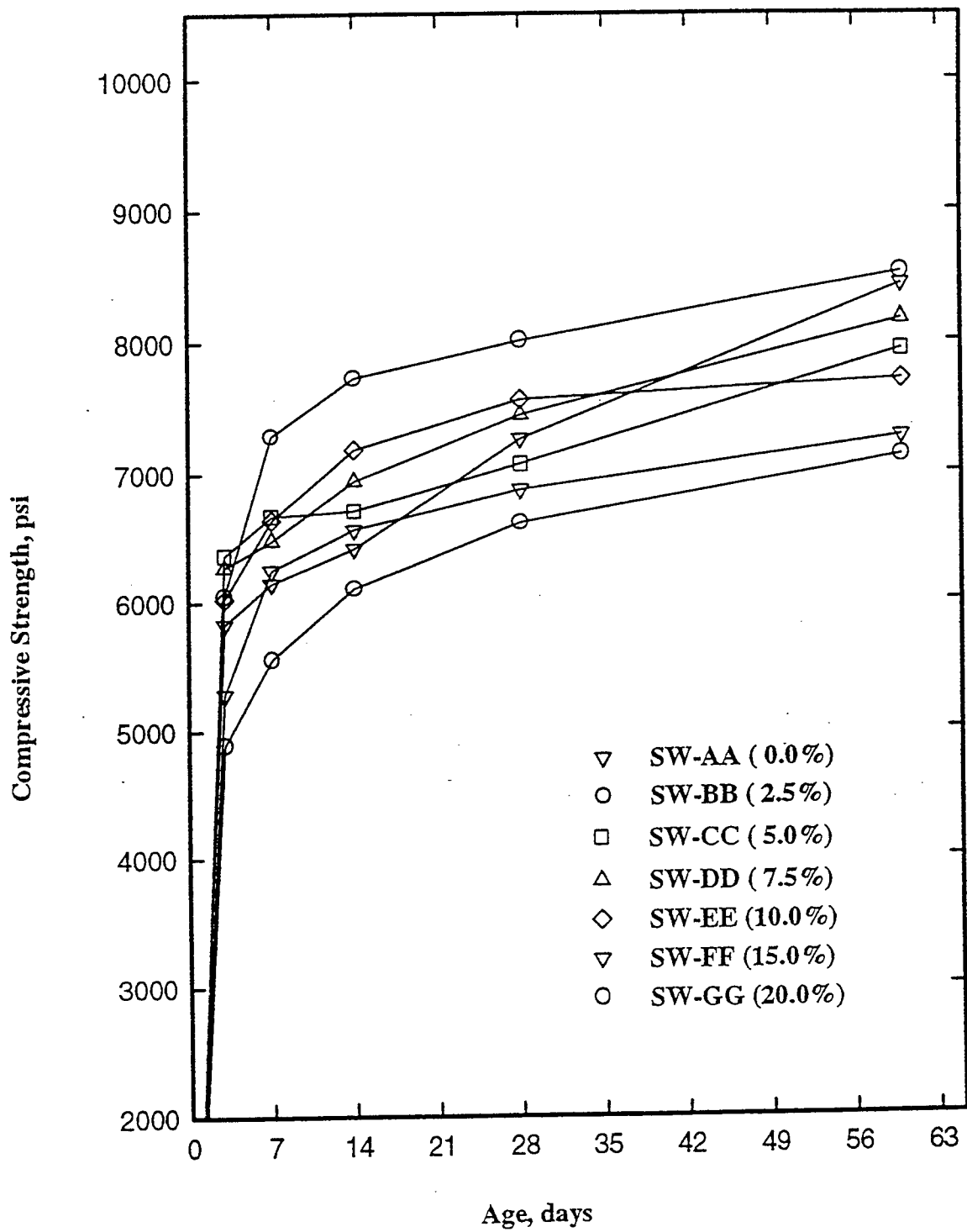


Figure 8. Compressive strengths of samples of cement-silica fume paste: SW-AA through SW-GG.

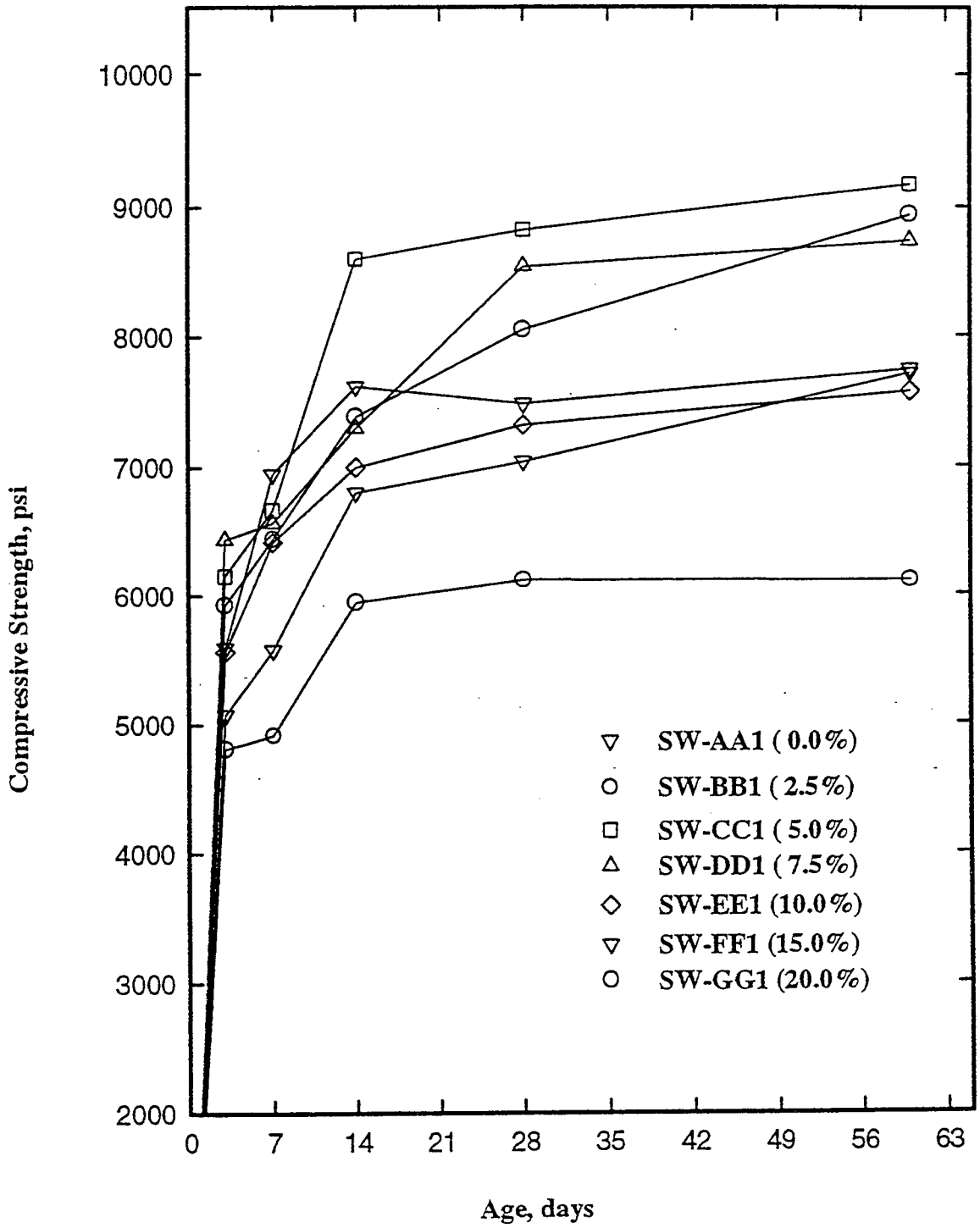


Figure 9. Compressive strengths of samples of cement-silica fume paste: SW-AA1 through SW-GG1.

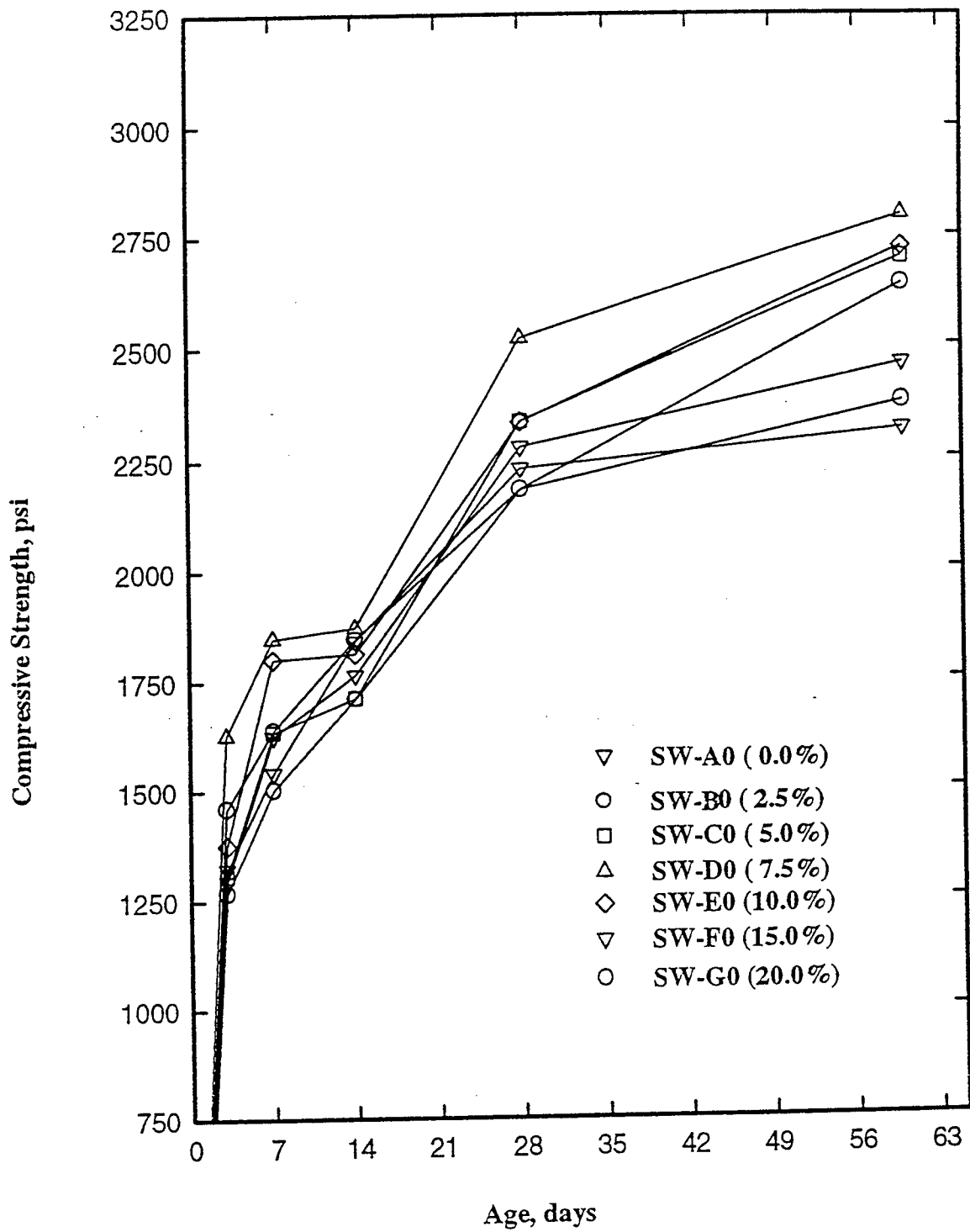


Figure 10. Compressive strengths of samples of cement-silica fume mortar: SW-A0 through SW-G0.

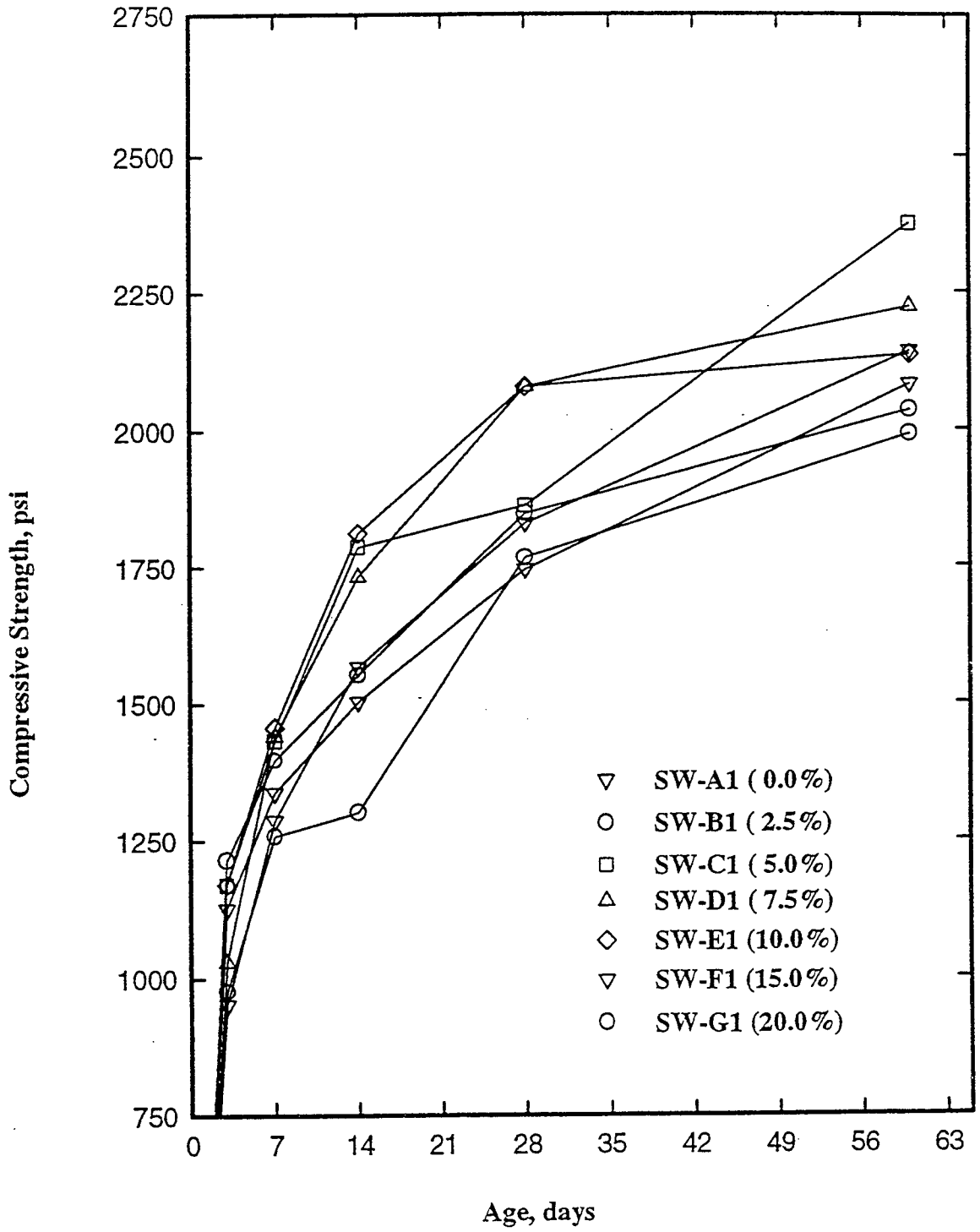
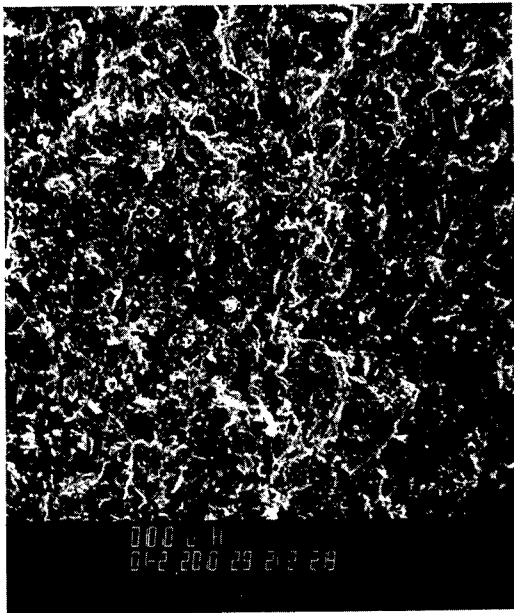
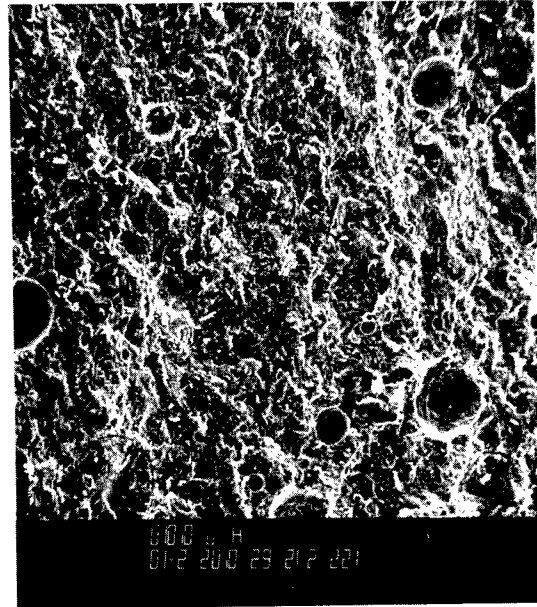


Figure 11. Compressive strengths of samples of cement-silica fume mortar: SW-A1 through SW-G1.



(i)



(ii)

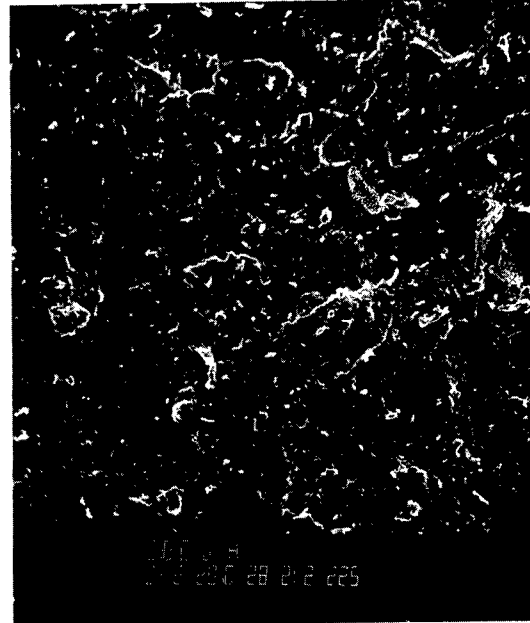
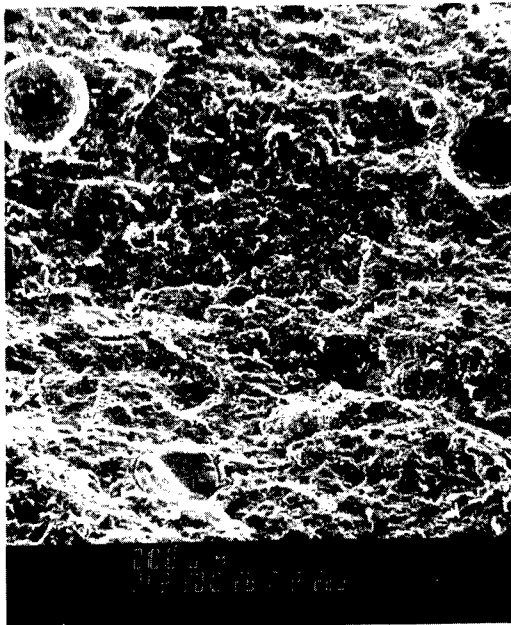
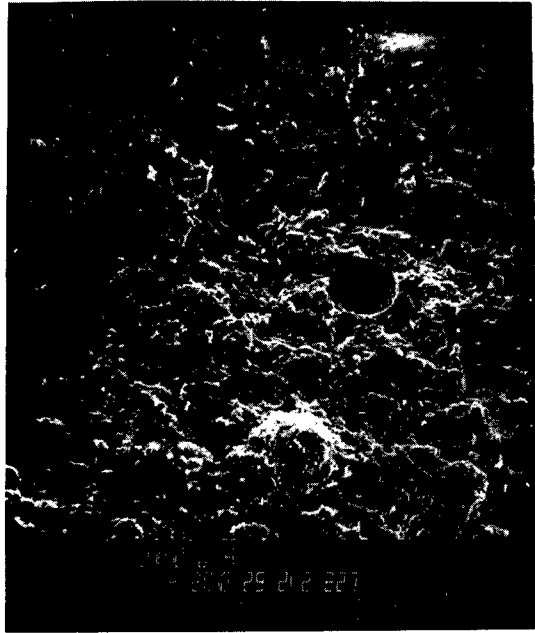


Figure 12a. SEM micrographs of samples of cement-silica fume paste (100X): (i) SW-AA; (ii) SW-BB; (iii) SW-CC; and (iv) SW-DD.



(v)

(vi)

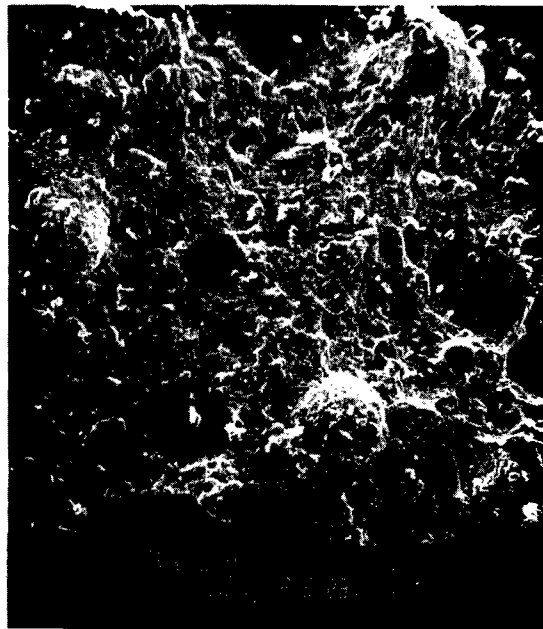
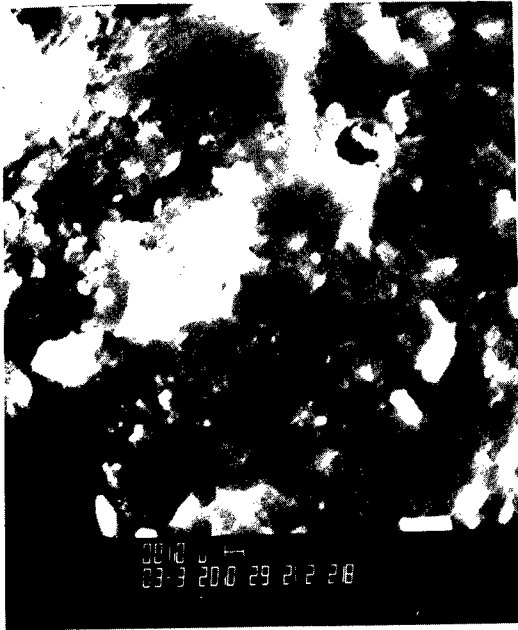


Figure 12b. SEM micrographs of samples of cement-silica fume paste (100X):
(v) SW-EE; (vi) SW-FF; and (vii) SW-GG.



(i)



(ii)

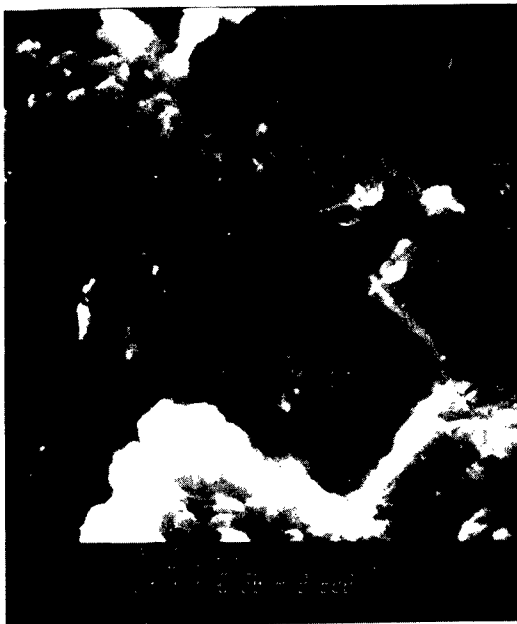


Figure 13a. SEM micrographs of samples of cement-silica fume paste (3,000X):
(i) SW-AA; (ii) SW-BB; (iii) SW-CC; and (iv) SW-DD.



(v)

(vi)

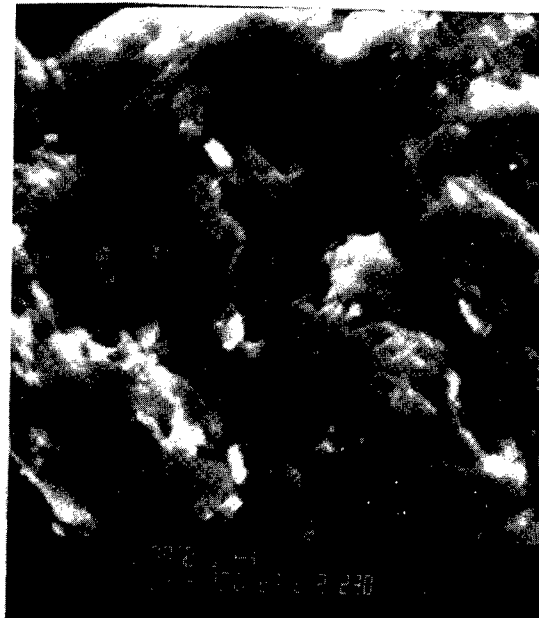
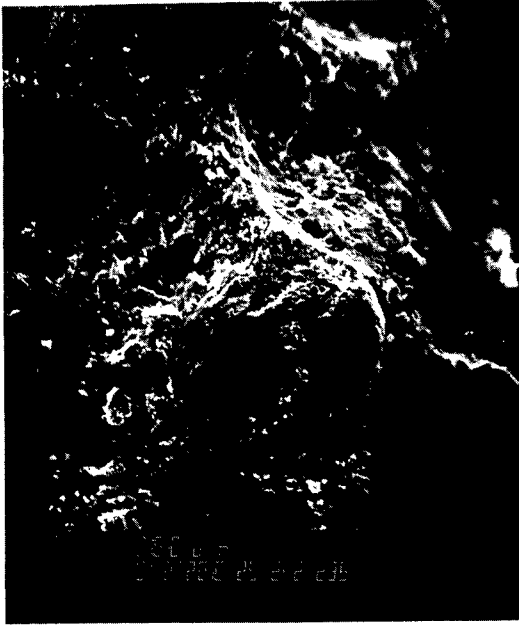


Figure 13b. SEM micrographs of samples of cement-silica fume paste (3,000X):
(v) SW-EE; (vi) SW-FF; and (vii) SW-GG.



(i)



(ii)

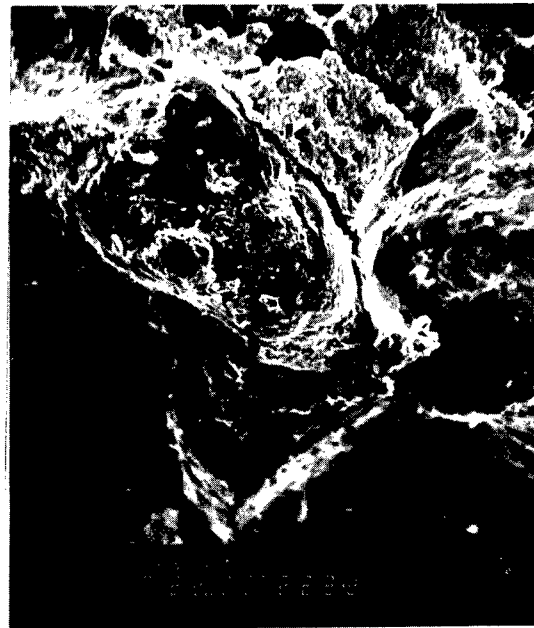
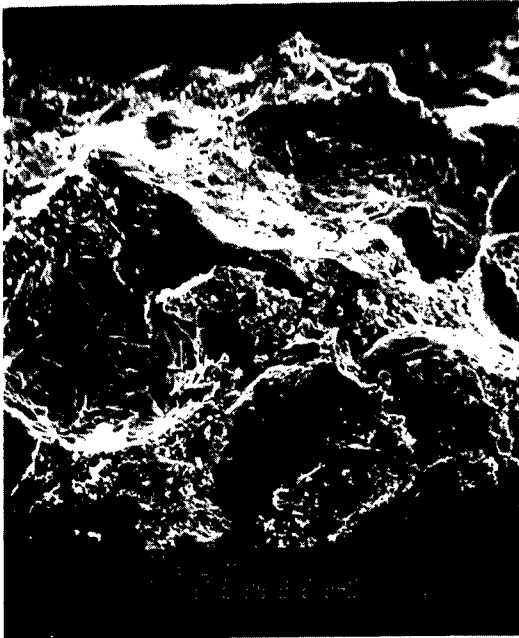
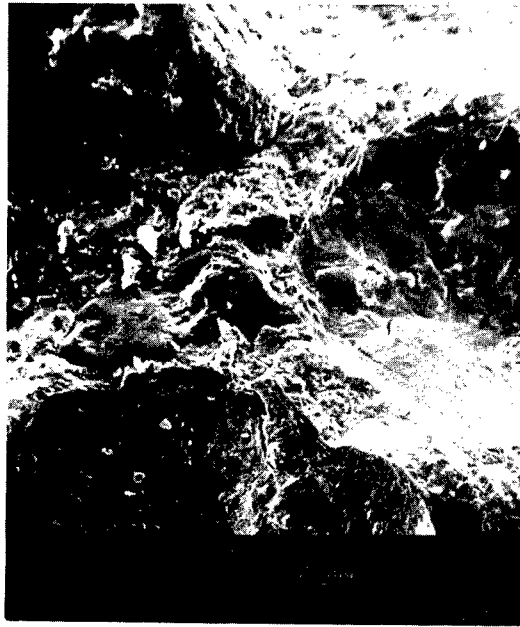


Figure 14a. SEM micrographs of samples of cement-silica fume mortar (100X):
(i) SW-A0; (ii) SW-B0; (iii) SW-C0; and (iv) SW-D0.



(v)

(vi)

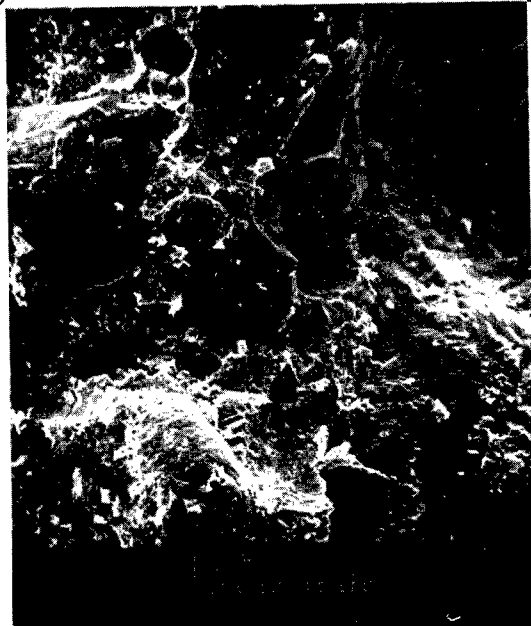


Figure 14b. SEM micrographs of samples of cement-silica fume mortar (100X):
(v) SW-E0; (vi) SW-F0; and (vii) SW-G0.



(i)



(ii)

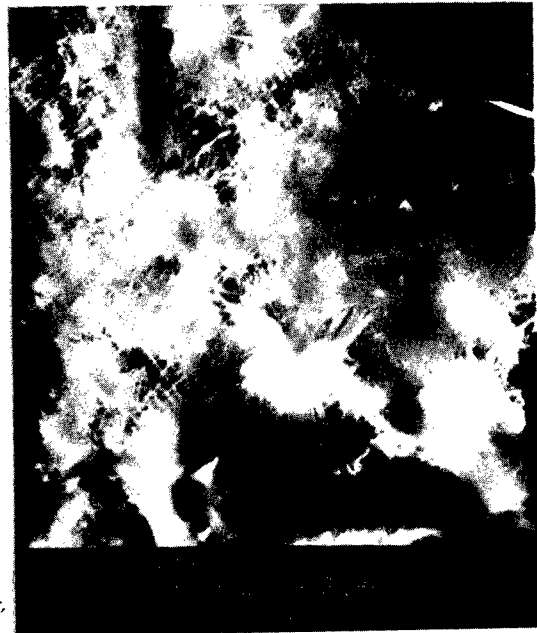
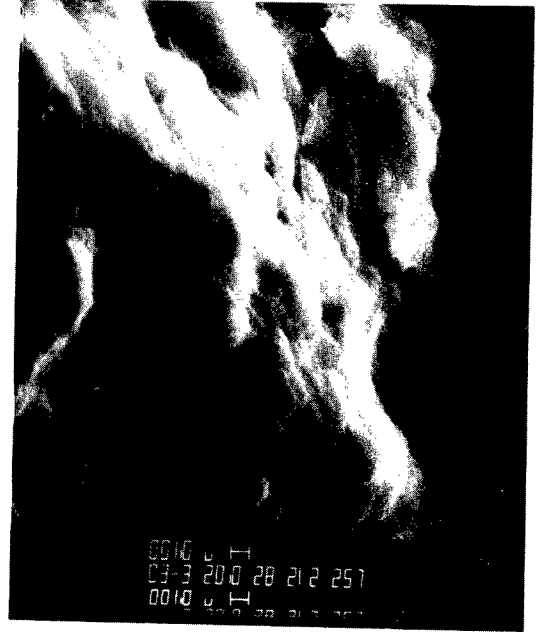


Figure 15a. SEM micrographs of samples of cement-silica fume mortar (3,000X):
(i) SW-A0; (ii) SW-B0; (iii) SW-C0; and (iv) SW-D0.



(v)



(vi)



Figure 15b. SEM micrographs of samples of cement-silica fume mortar (3,000X):
(v) SW-E0; (vi) SW-F0; and (vii) SW-G0.



Figure 16a. SEM micrograph of sample S-1 of cement-silica fume paste (10,000X): Area 1.



Figure 16b. SEM micrograph of sample S-1 of cement-silica fume paste (10,000X):
Area 2.

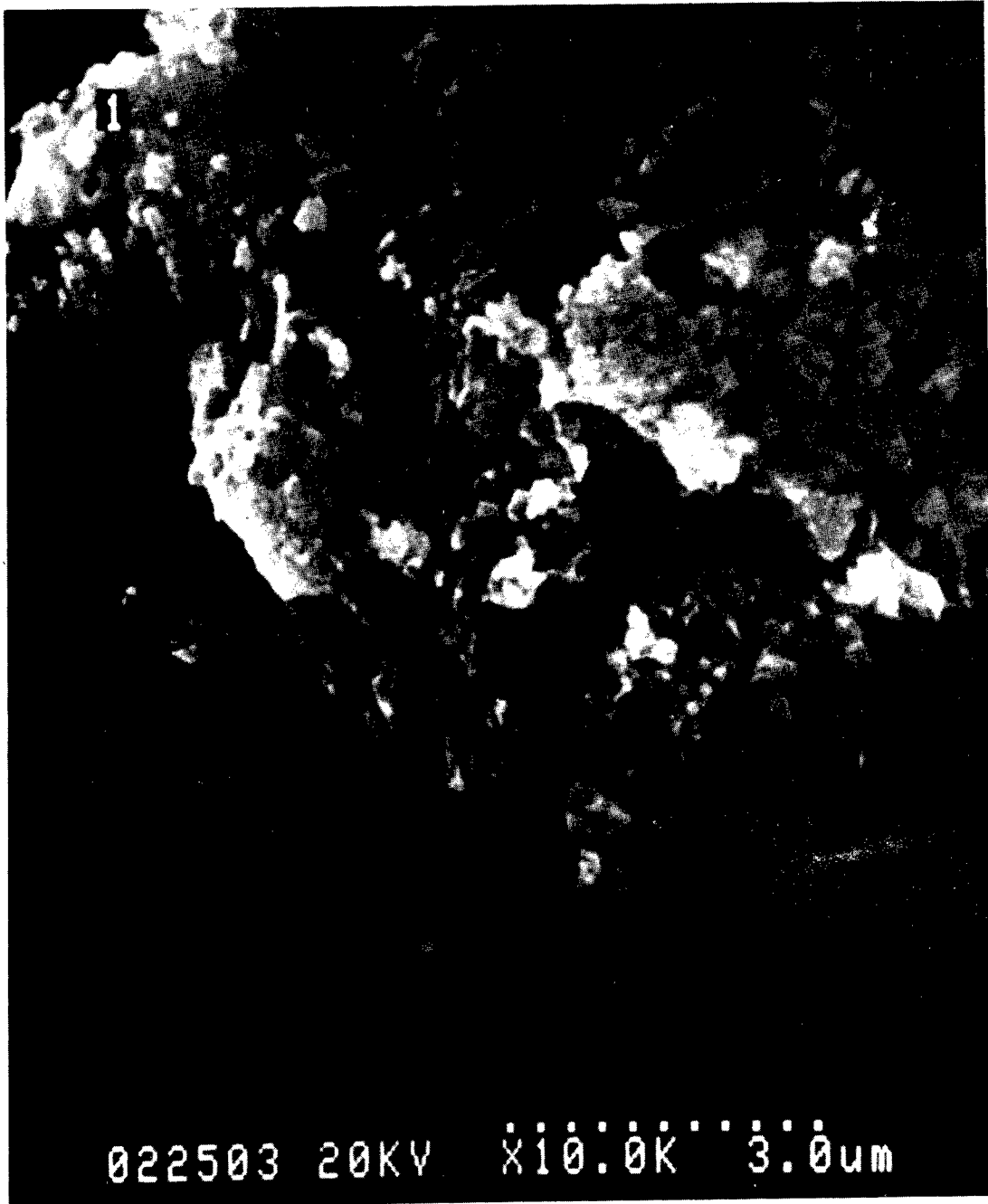


Figure 16c. SEM micrograph of sample S-1 of cement-silica fume paste (10,000X): Area 3.

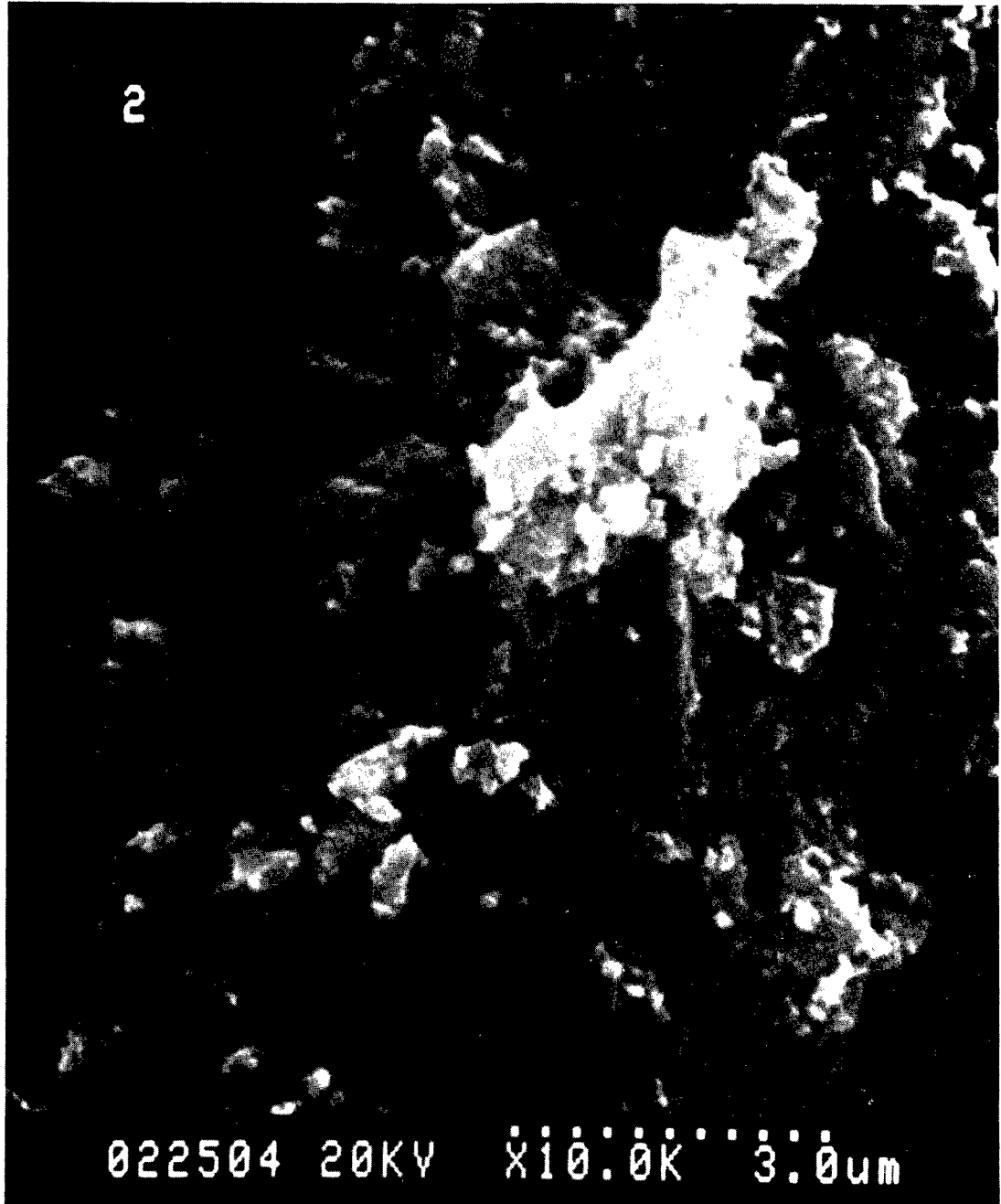


Figure 17a. SEM micrograph of sample S-2 of cement-silica fume paste (10,000X): Area 1.

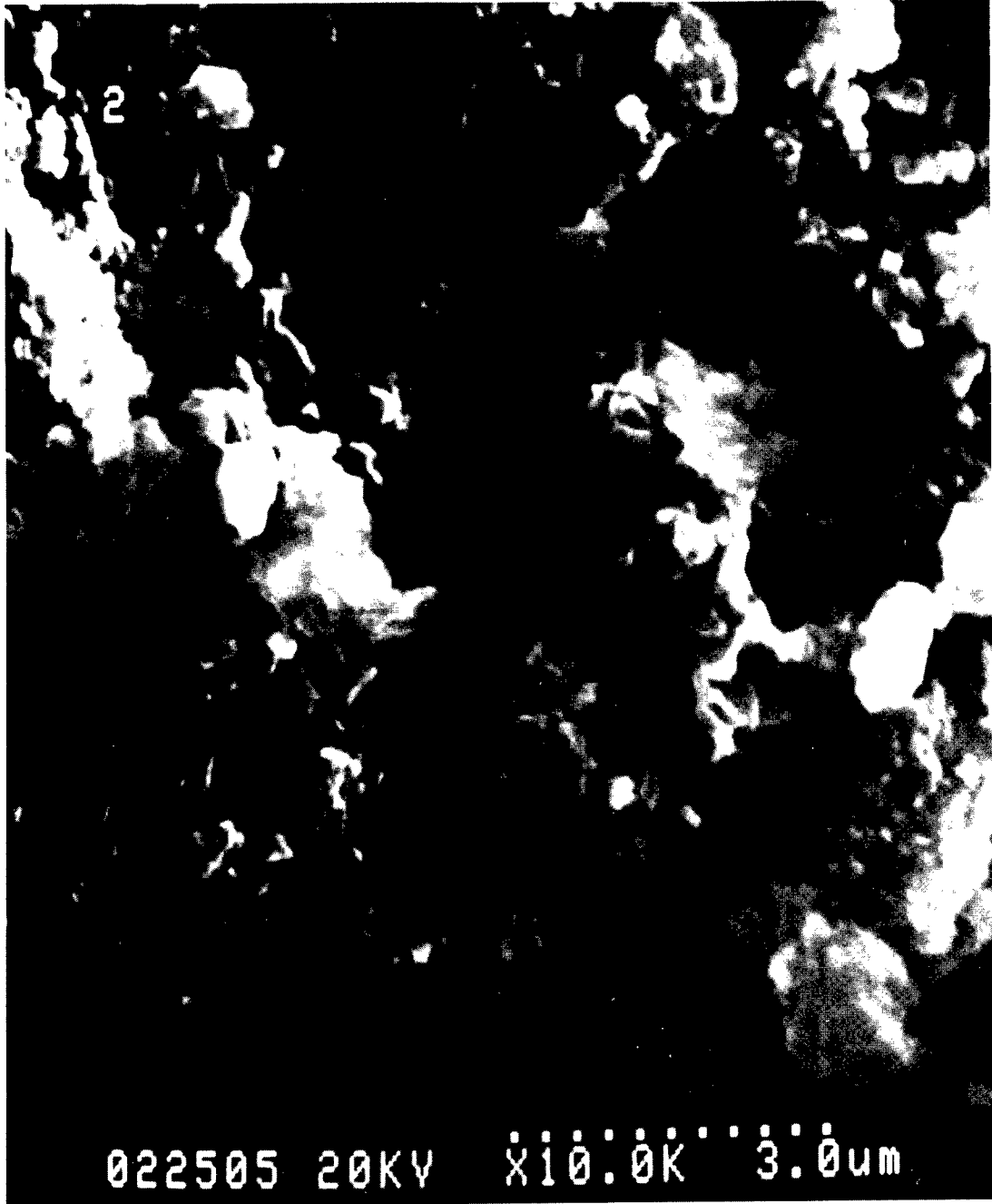


Figure 17b. SEM micrograph of sample S-2 of cement-silica fume paste (10,000X):
Area 2.

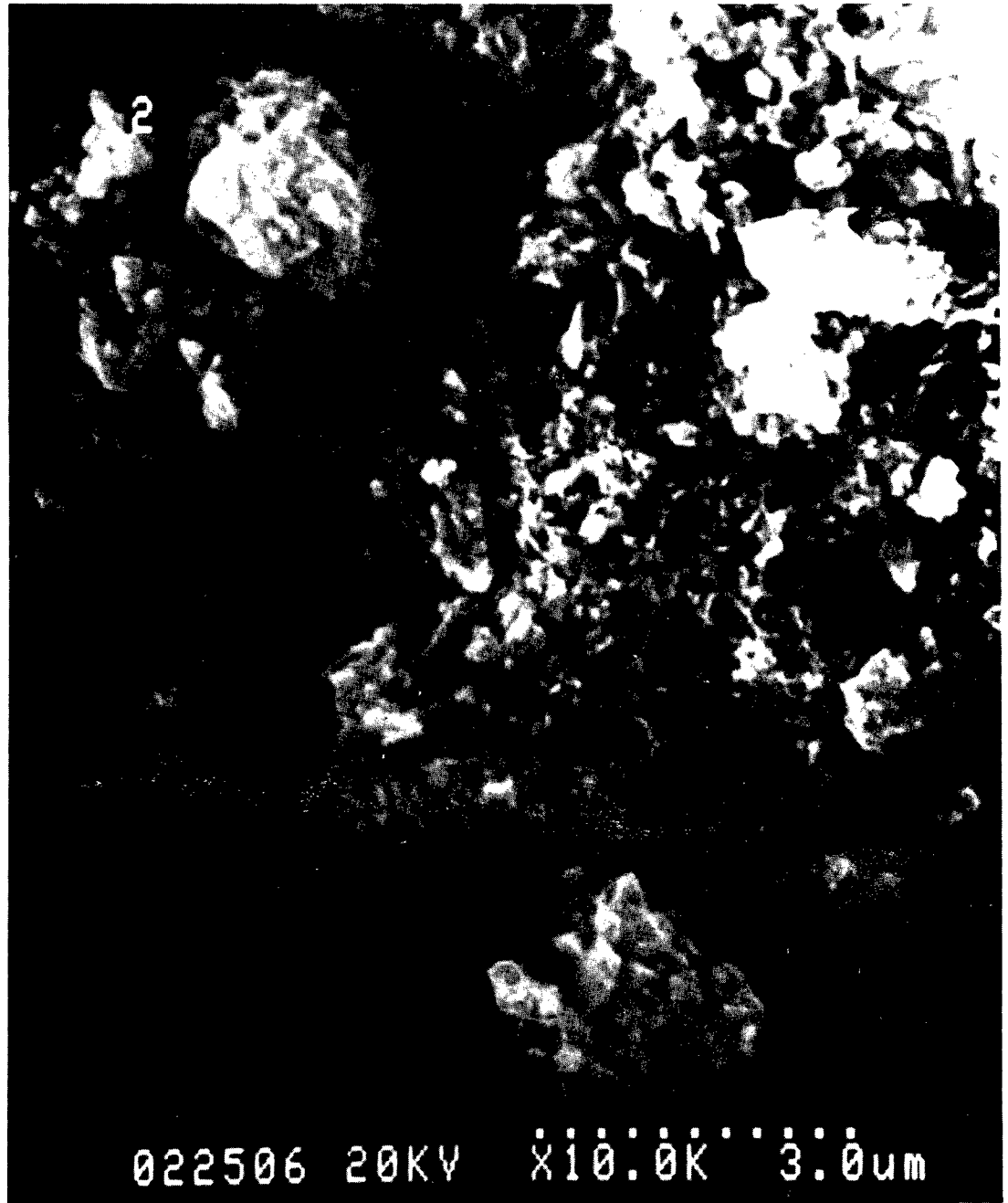


Figure 17c. SEM micrograph of sample S-2 of cement-silica fume paste (10,000X): Area 3.



Figure 18a. SEM micrograph of sample S-3 of cement-silica fume paste (10,000X): Area 1.



Figure 18b. SEM micrograph of sample S-3 of cement-silica fume paste (10,000X): Area 2.



Figure 18c. SEM micrograph of sample S-3 of cement-silica fume paste (10,000X): Area 3.

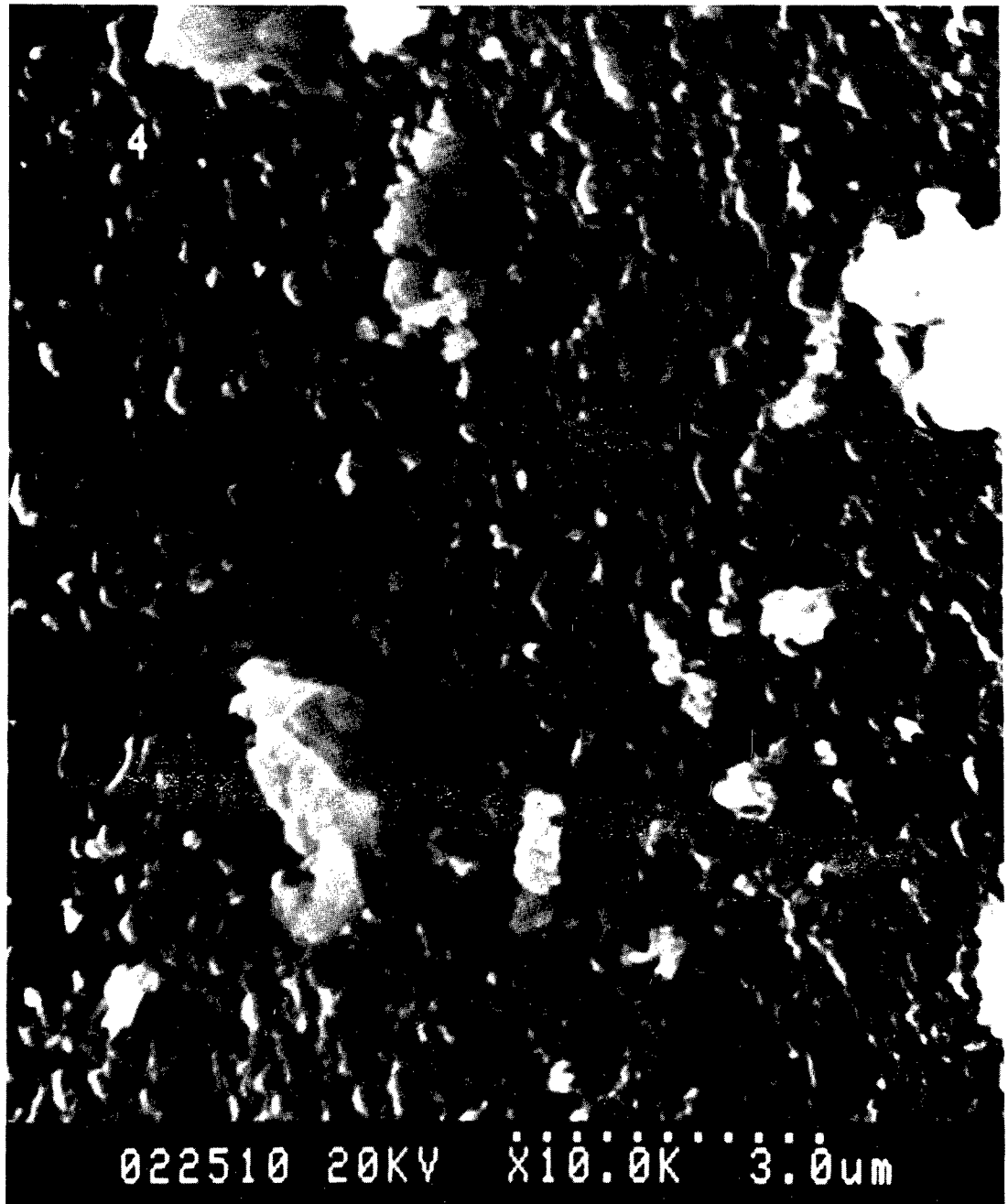


Figure 19a. SEM micrograph of sample S-4 of cement-silica fume paste (10,000X): Area 1.



Figure 19b. SEM micrograph of sample S-4 of cement-silica fume paste (10,000X):
Area 2.



Figure 19c. SEM micrograph of sample S-4 of cement-silica fume paste (10,000X): Area 3.



Figure 20a. SEM micrograph of sample S-5 of cement-silica fume paste (10,000X): Area 1.



Figure 20b. SEM micrograph of sample S-5 of cement-silica fume paste (10,000X): Area 2.



Figure 20c. SEM micrograph of sample S-5 of cement-silica fume paste (10,000X): Area 3.



Figure 21a. SEM micrograph of sample S-6 of cement-silica fume paste (10,000X):
Area 1.



Figure 21b. SEM micrograph of sample S-6 of cement-silica fume paste (10,000X): Area 2.



Figure 21c. SEM micrograph of sample S-6 of cement-silica fume paste (10,000X): Area 3.



Figure 22a. SEM micrograph of sample S-7 of cement-silica fume paste (10,000X): Area 1.



Figure 22b. SEM micrograph of sample S-7 of cement-silica fume paste (10,000X): Area 2.



Figure 22c. SEM micrograph of sample S-7 of cement-silica fume paste (10,000X): Area 3.

Sample: A:1D
 Data file: A:1D.RAW

14-Feb-1995 15:07:22

Seq	2theta	d	rel. I	Seq	2theta	d	rel. I
1	18.008	4.9229	100.00	1	18.008	4.9229	100.00
2	22.847	3.8900	28.31	4	34.047	2.6317	53.59
3	29.435	3.0326	34.38	3	29.435	3.0326	34.38
4	34.047	2.6317	53.59	5	47.113	1.9278	30.84
5	47.113	1.9278	30.84	2	22.847	3.8900	28.31

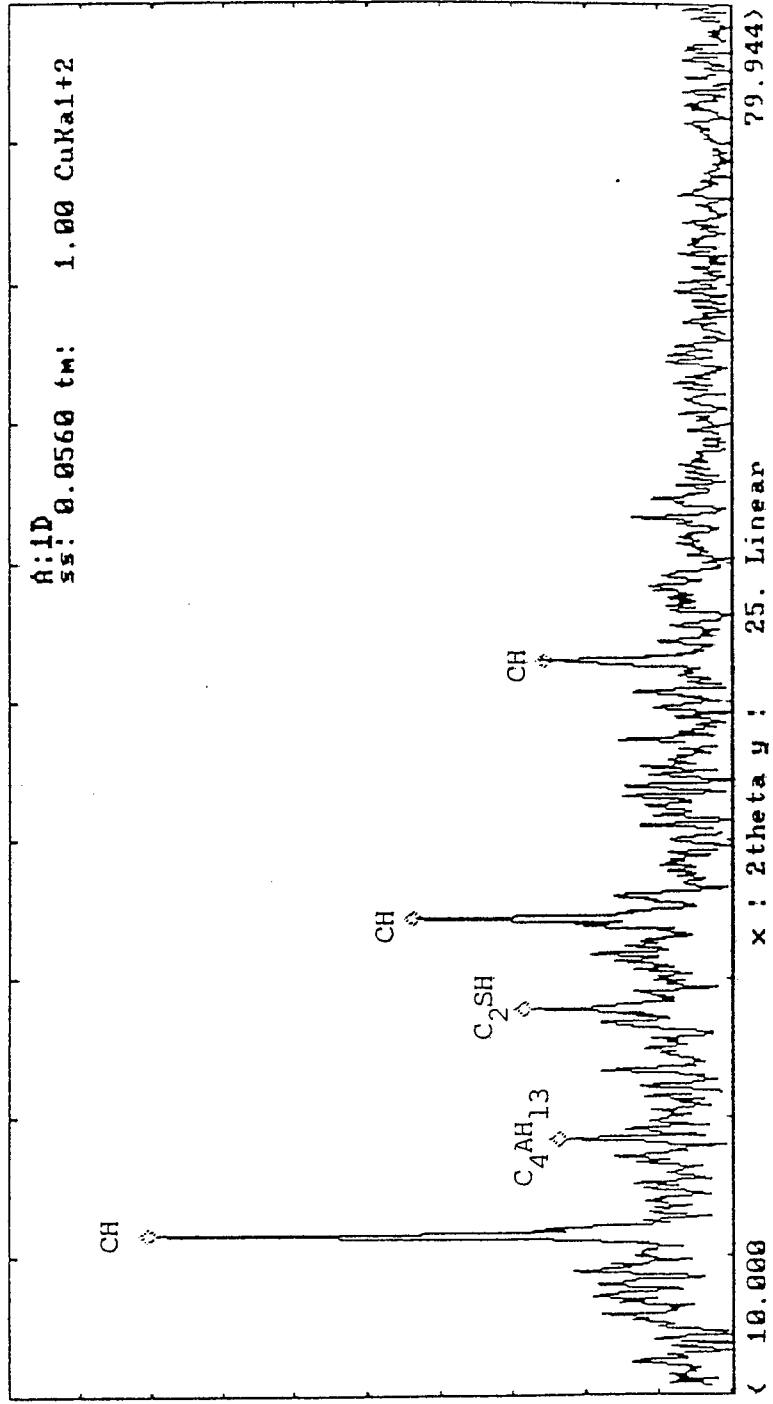


Figure 23. XRD pattern of sample S-1 of cement-silica fume paste.

14-Feb-1995 16:22:41

Sample: A:2D
Data file: A:2D.RAW

Seq	2theta	d	rel. I	Seq	2theta	d	rel. I
1	17.906	4.9508	100.00	1	17.906	4.9508	100.00
2	18.235	4.8621	48.54	4	34.013	2.6342	74.34
3	29.435	3.0326	28.64	2	18.235	4.8621	48.54
4	34.013	2.6342	74.34	3	29.435	3.0326	28.64
5	47.113	1.9278	23.79	5	47.113	1.9278	23.79
6	51.505	1.7732	19.42	6	51.505	1.7732	19.42

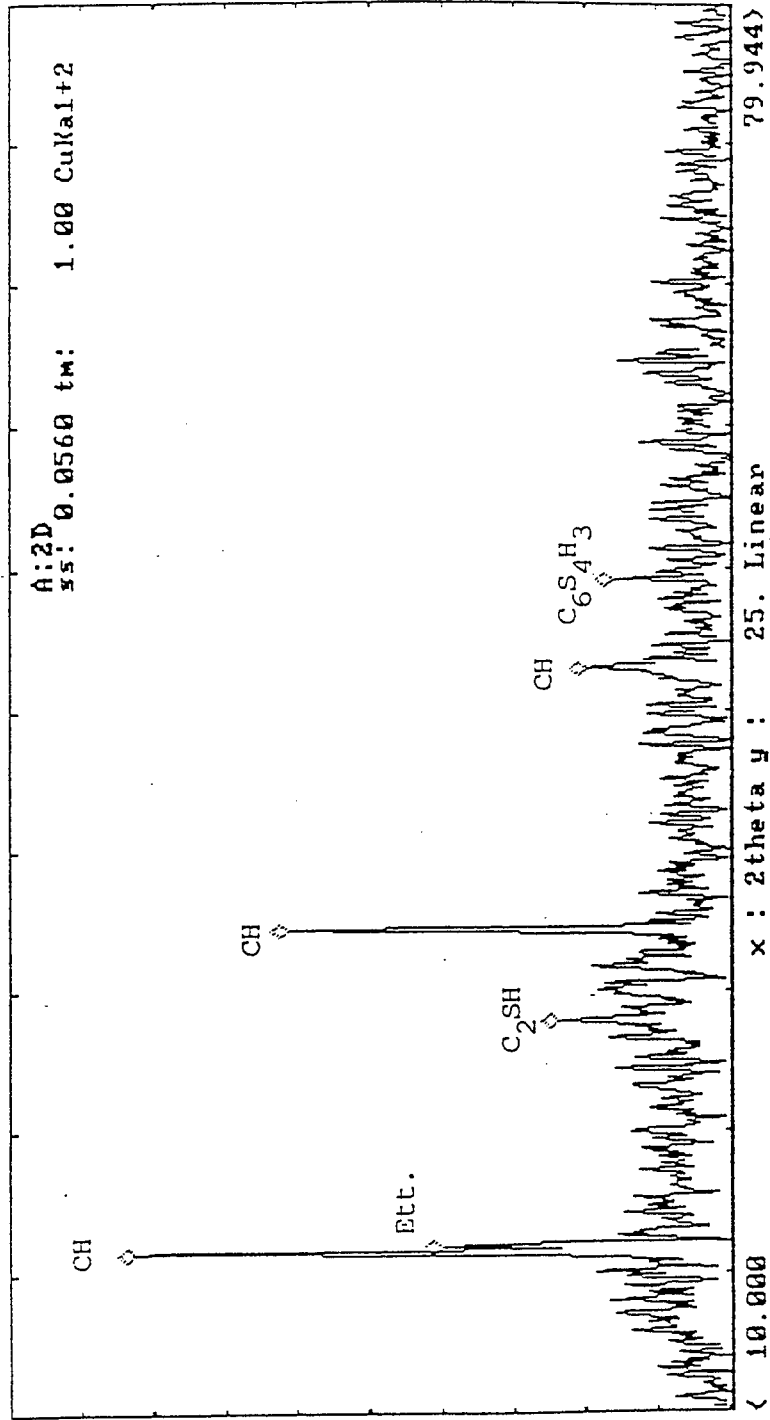


Figure 24. XRD pattern of sample S-2 of cement-silica fume paste.

Sample: A:4D
 Data file: A:4D.RAW
 14-Feb-1995 16:30:11

Seq	2theta	d	rel. I	Seq	2theta	d	rel. I
1	17.972	4.9328	100.00	1	17.972	4.9328	100.00
2	18.345	4.8332	45.71	6	34.047	2.6317	73.02
3	28.666	3.1122	41.40	5	32.180	2.7799	67.44
4	29.325	3.0437	44.65	7	47.113	1.9278	47.91
5	32.180	2.7799	67.44	2	18.345	4.8332	45.71
6	34.047	2.6317	73.02	4	29.325	3.0437	44.65
7	47.113	1.9278	47.91	3	28.666	3.1122	41.40
8	49.639	1.8355	31.16	8	49.639	1.8355	31.16

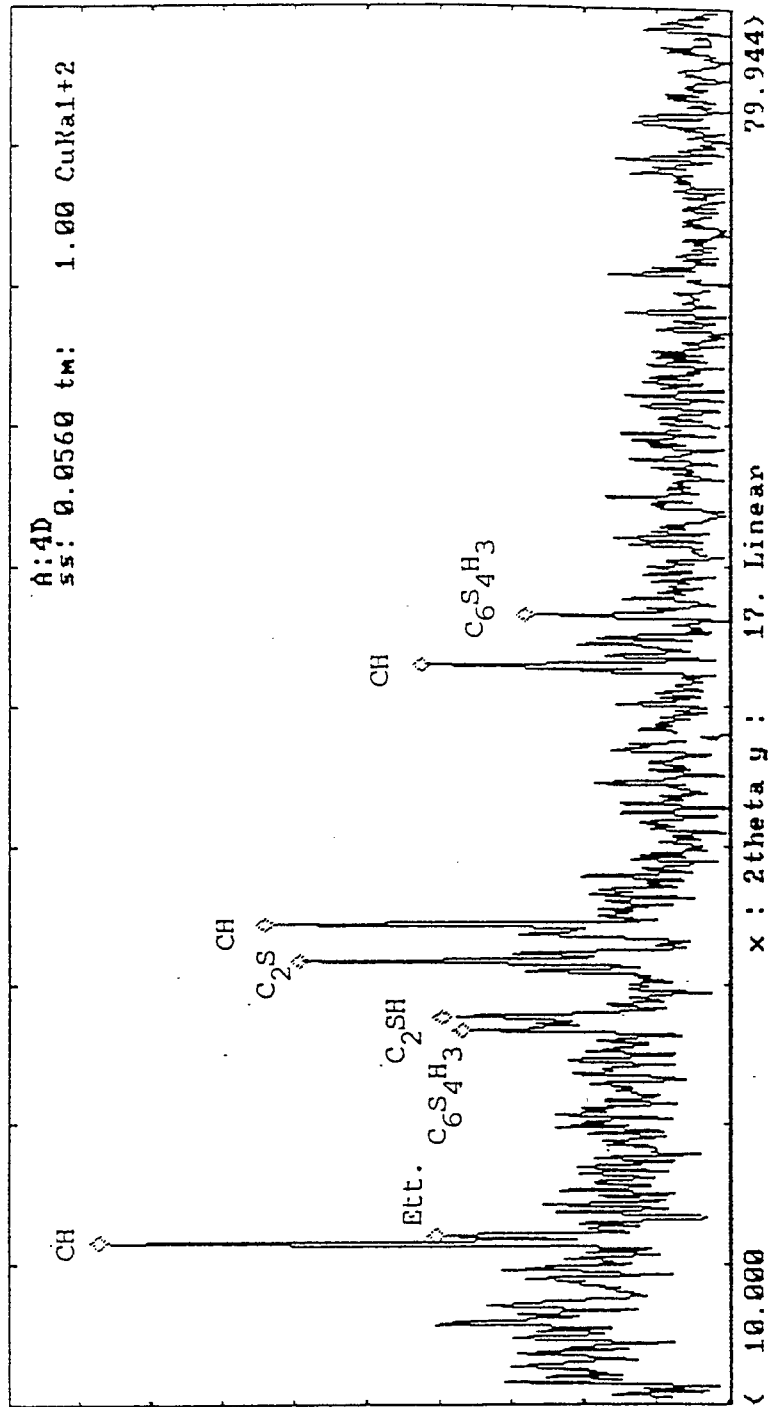


Figure 26. XRD pattern of sample S-4 of cement-silica fume paste.

Sample: A:3D
 Data file: A:3D.RAW
 14-Feb-1995 16:26:09

Seq	2theta	d	rel. I	Seq	2theta	d	rel. I
1	11.647	7.5933	43.17	2	17.929	4.9444	100.00
2	17.929	4.9444	100.00	1	11.647	7.5933	43.17
3	22.847	3.8900	34.28	4	33.975	2.6371	40.56
4	33.975	2.6371	40.56	3	22.847	3.8900	34.28
5	38.109	2.3599	29.32	5	38.109	2.3599	29.32
6	47.113	1.9278	26.34	6	47.113	1.9278	26.34

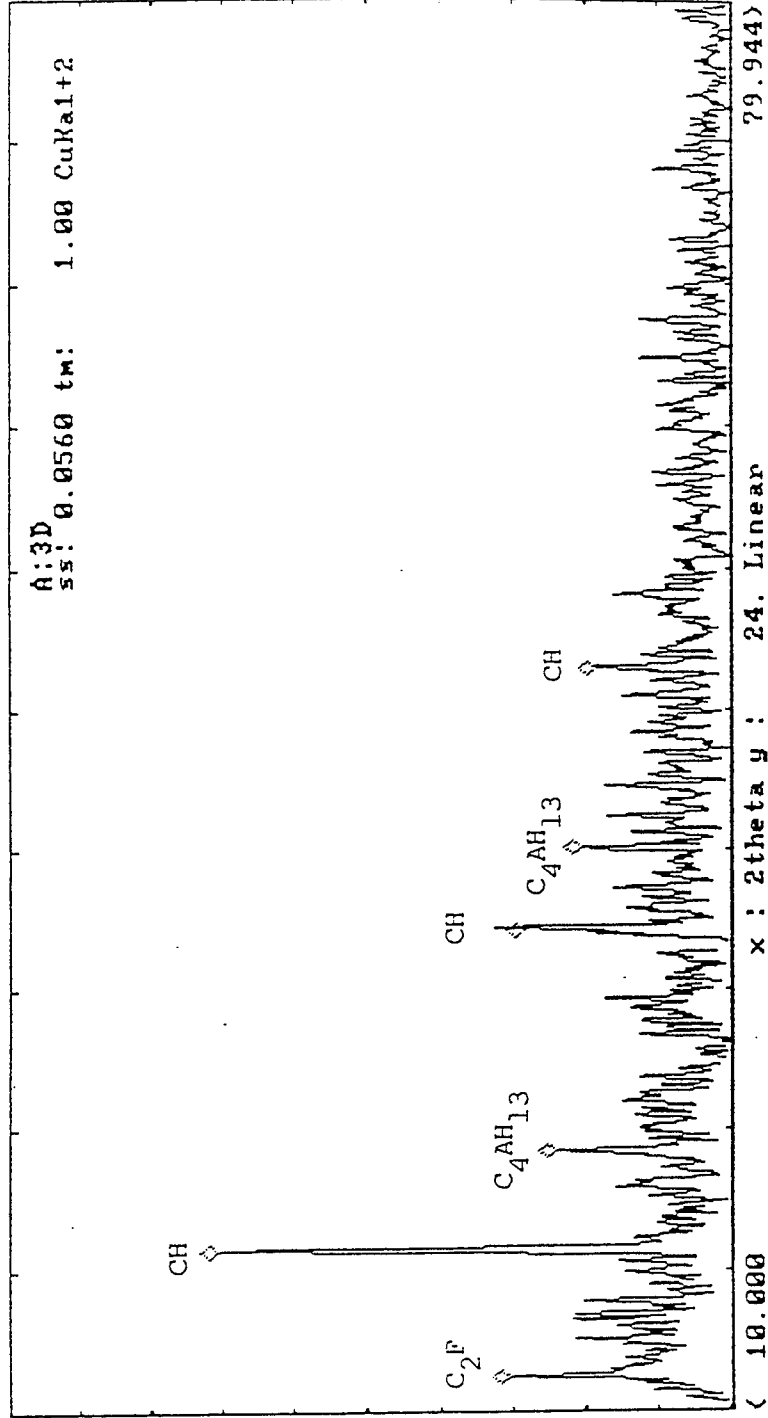


Figure 25. XRD pattern of sample S-3 of cement-silica fume paste.

Sample: A:5D
 Data file: A:5D.RAW
 14-Feb-1995 17:06:25

Seq	2theta	d	rel. I	Seq	2theta	d	rel. I
1	17.906	4.9508	100.00	1	17.906	4.9508	100.00
2	28.557	3.1239	33.62	3	33.937	2.6399	34.76
3	33.937	2.6399	34.76	2	28.557	3.1239	33.62

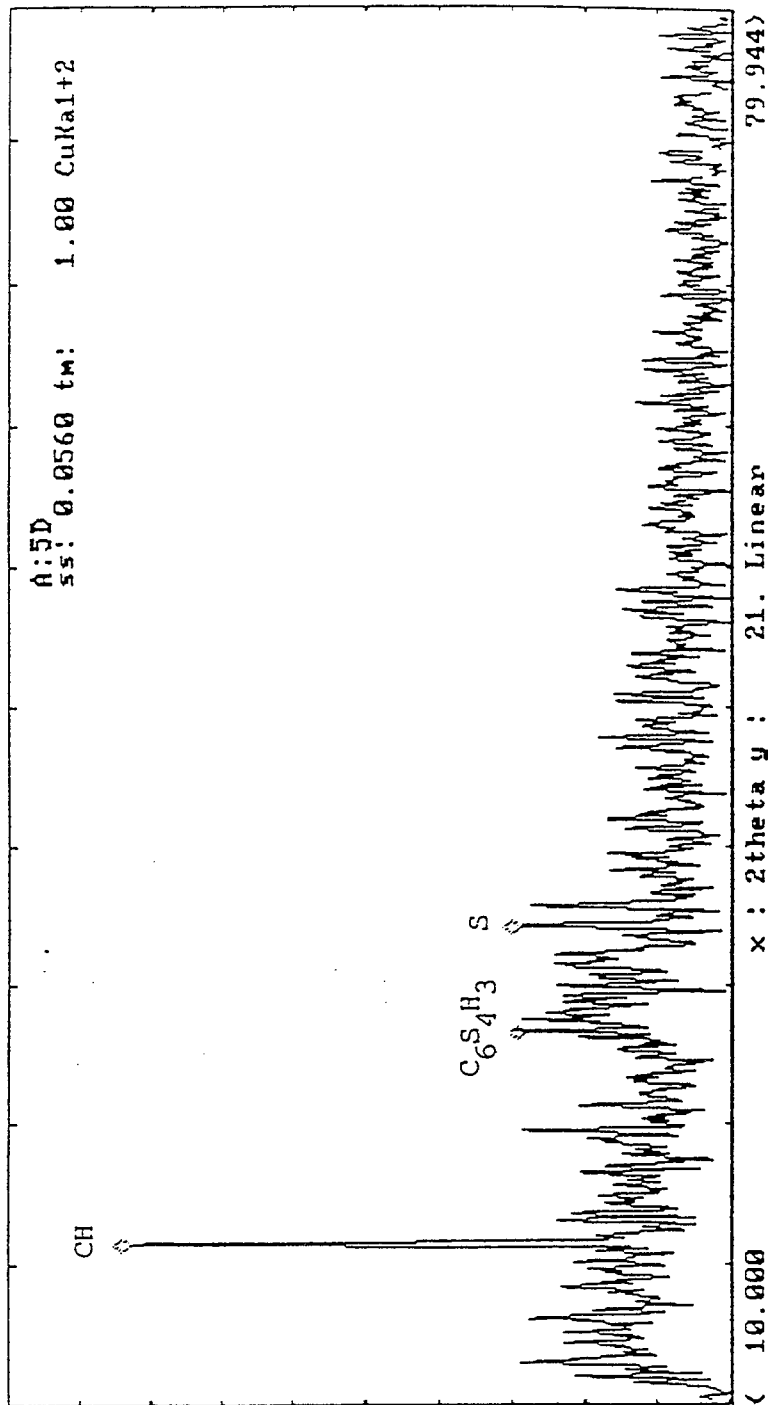


Figure 27. XRD pattern of sample S-5 of cement-silica fume paste.

14-Feb-1995 17:09:53

Sample: A:6D
Data file: A:6D.RAW

Seq	2theta	d	rel. I	Seq	2theta	d	rel. I
1	17.906	4.9508	100.00	1	17.906	4.9508	100.00
2	29.215	3.0549	76.62	2	29.215	3.0549	76.62
3	32.180	2.7799	63.76	4	34.047	2.6317	64.98
4	34.047	2.6317	64.98	3	32.180	2.7799	63.76

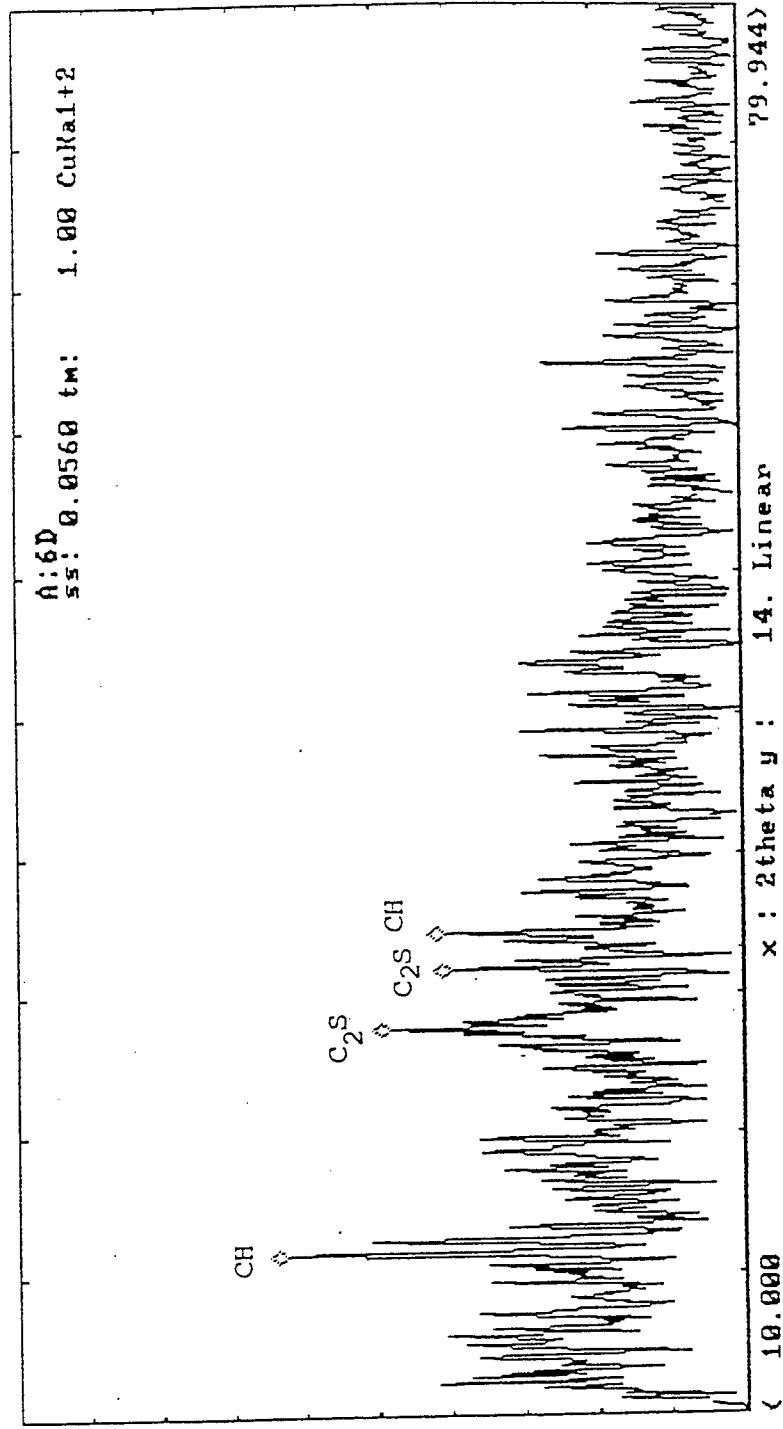


Figure 28. XRD pattern of sample S-6 of cement-silica fume paste.

Sample: A:7D
 Data file: A:7D.RAW
 22-Feb-1995 09:06:54

Seq	2theta	d	rel. I	Seq	2theta	d	rel. I
1	20.321	4.3674	100.00	1	20.321	4.3674	100.00
2	56.007	1.6409	56.60	2	56.007	1.6409	56.60

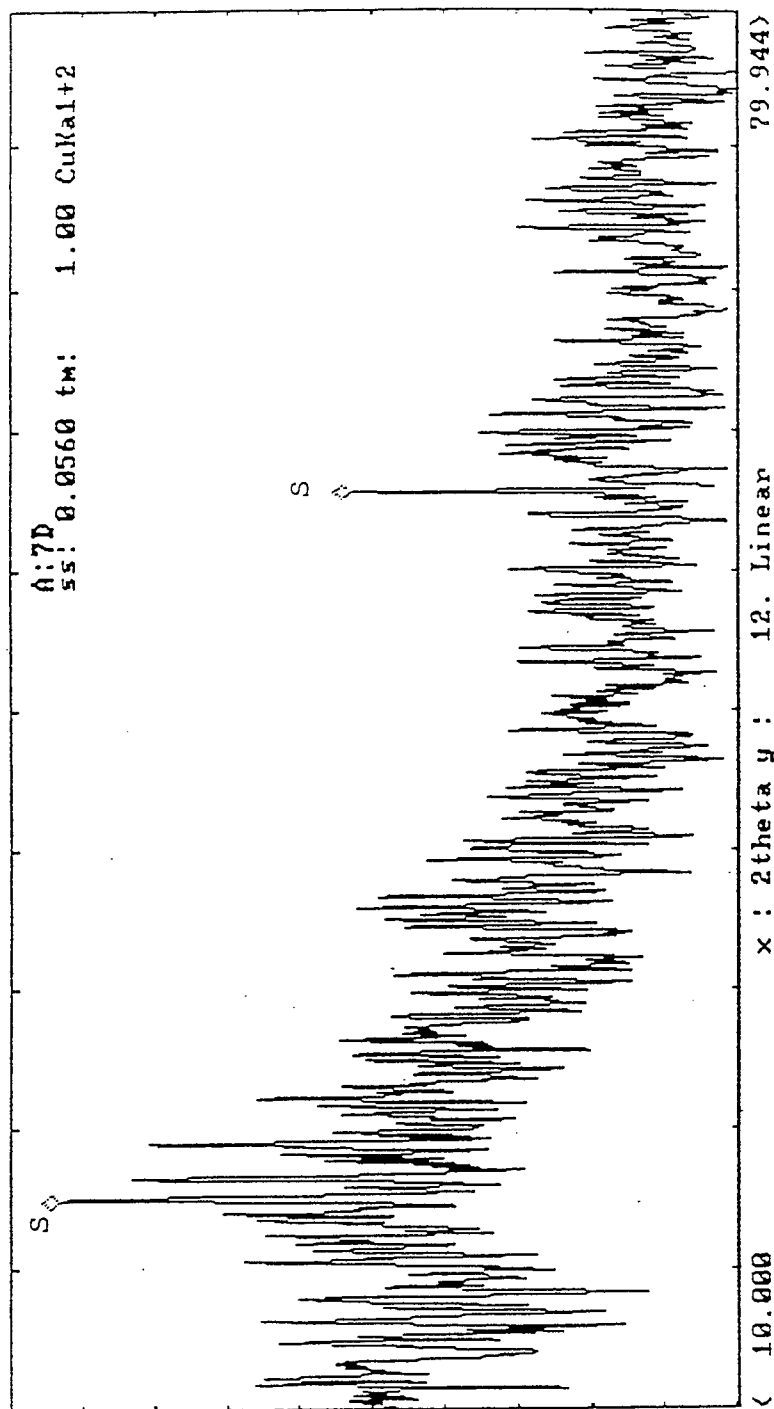


Figure 29. XRD pattern of sample S-7 of cement-silica fume paste.

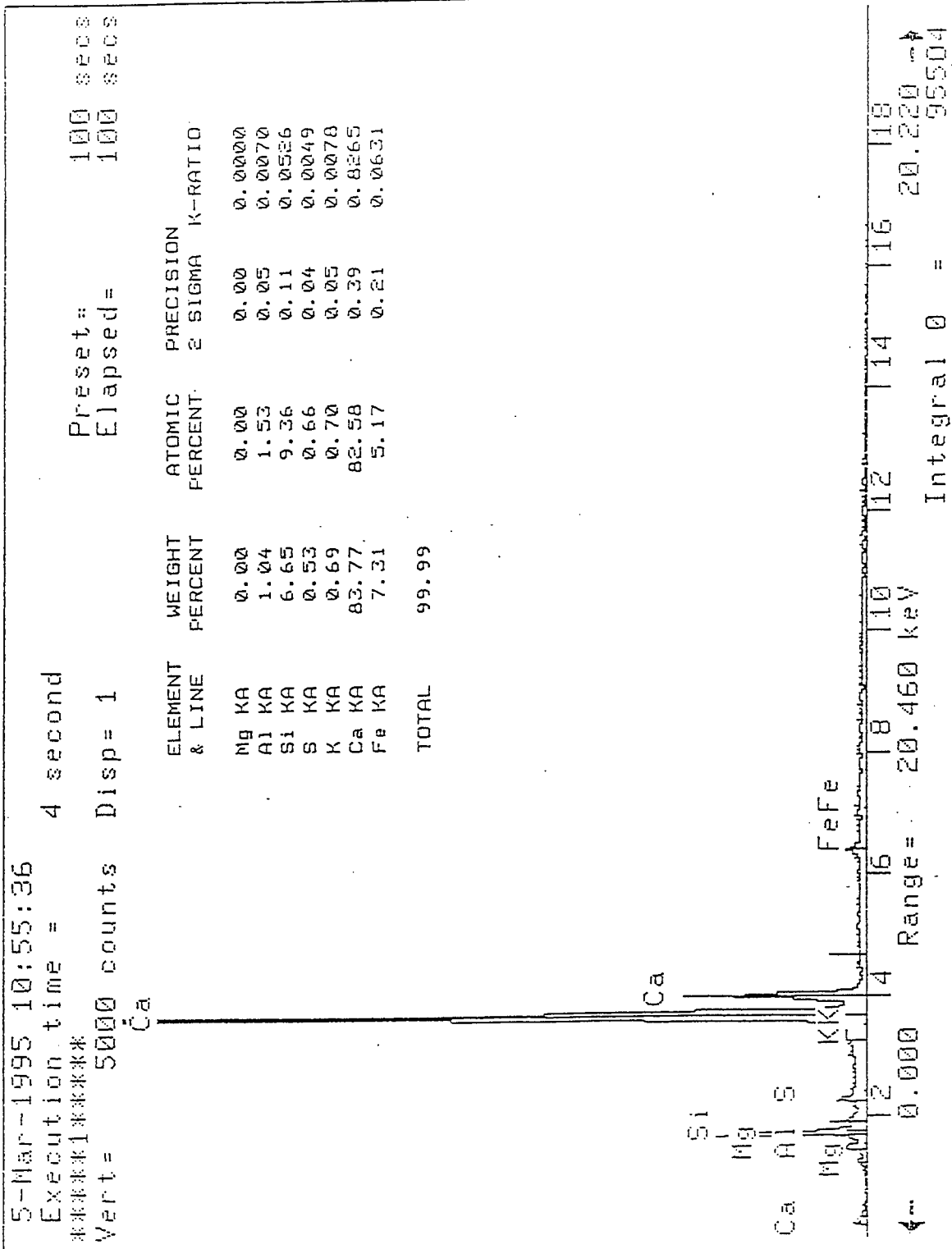


Figure 30. EDS spectrum of sample S-1 of cement-silica fume paste.

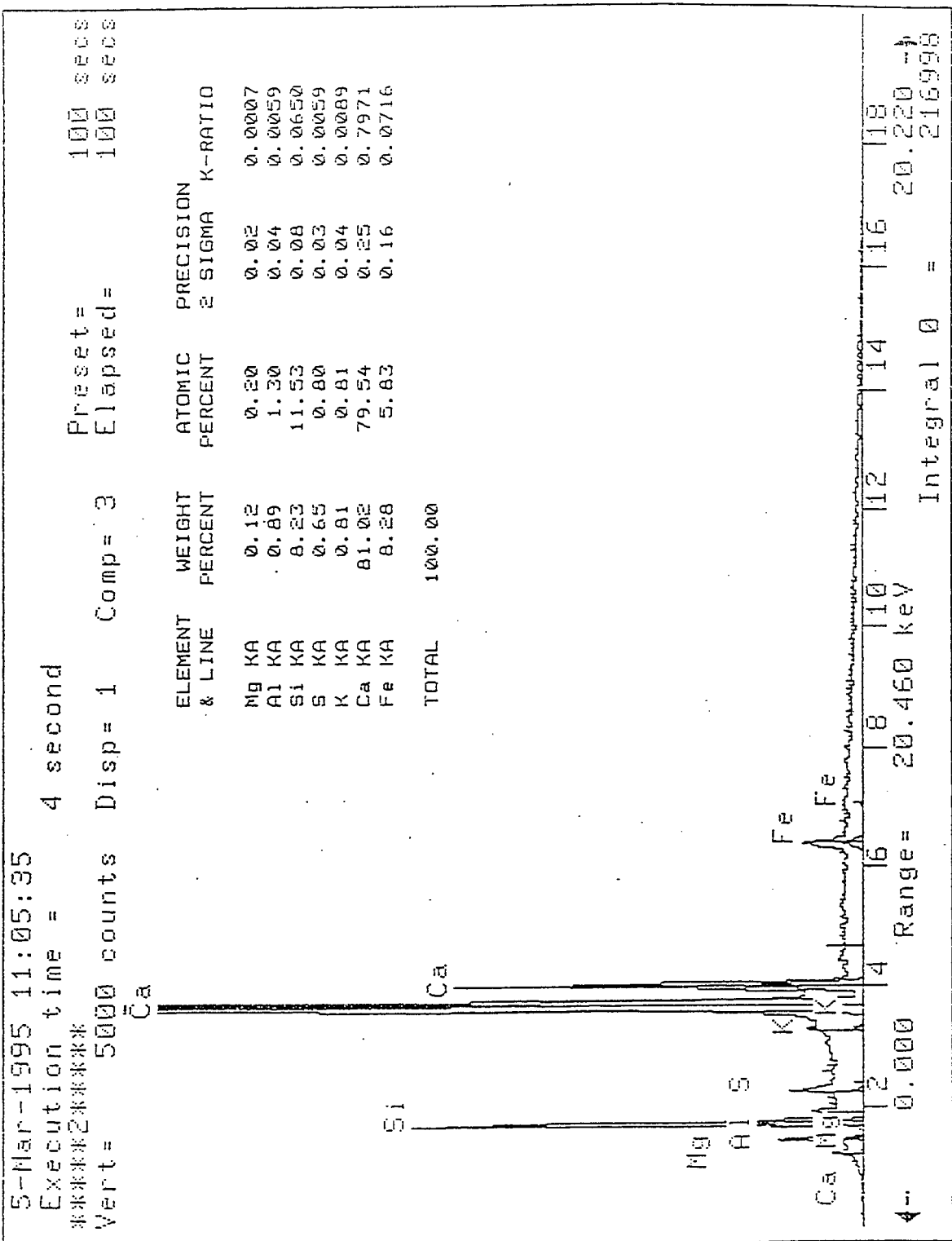


Figure 31. EDS spectrum of sample S-2 of cement-silica fume paste.

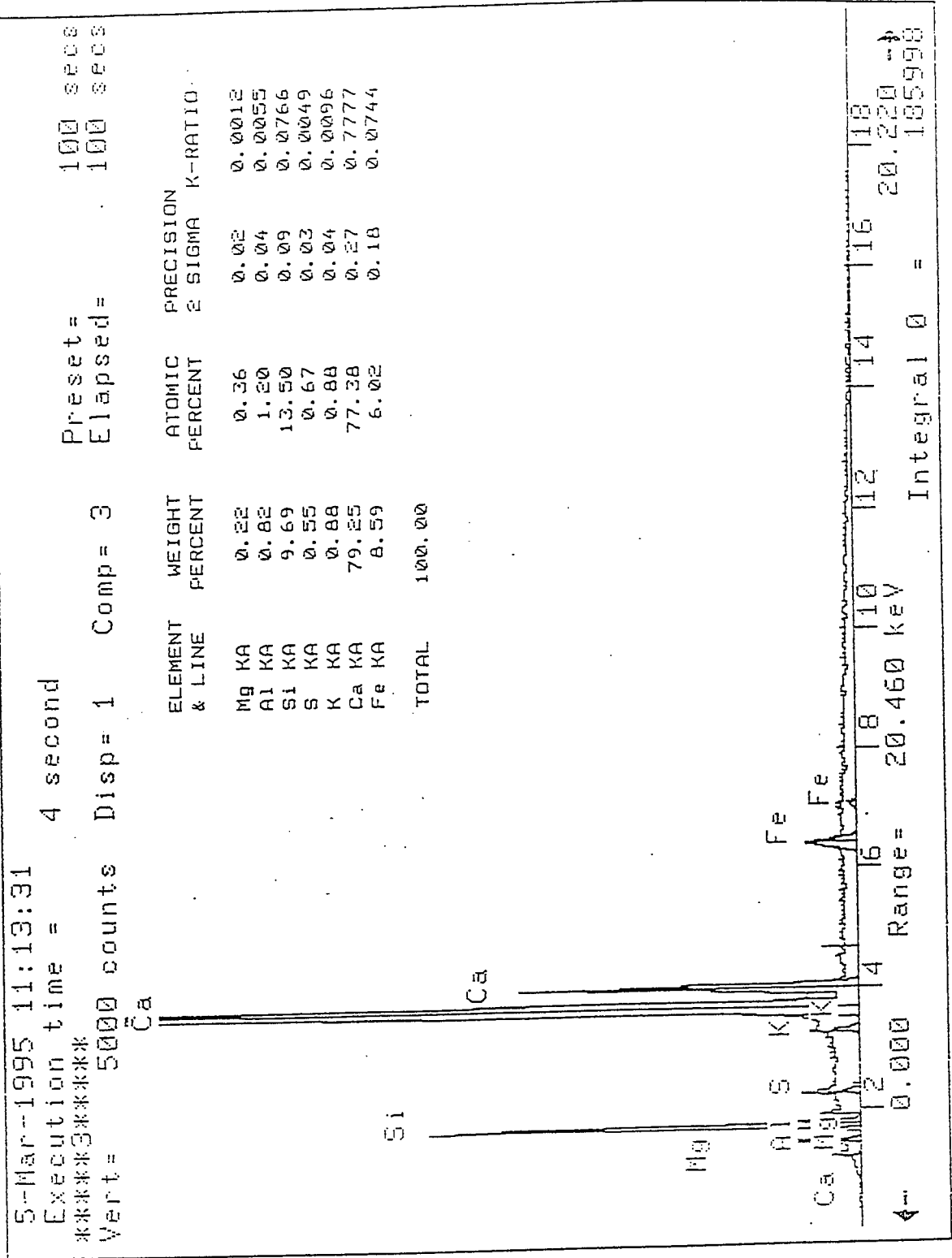


Figure 32. EDS spectrum of sample S-3 of cement-silica fume paste.

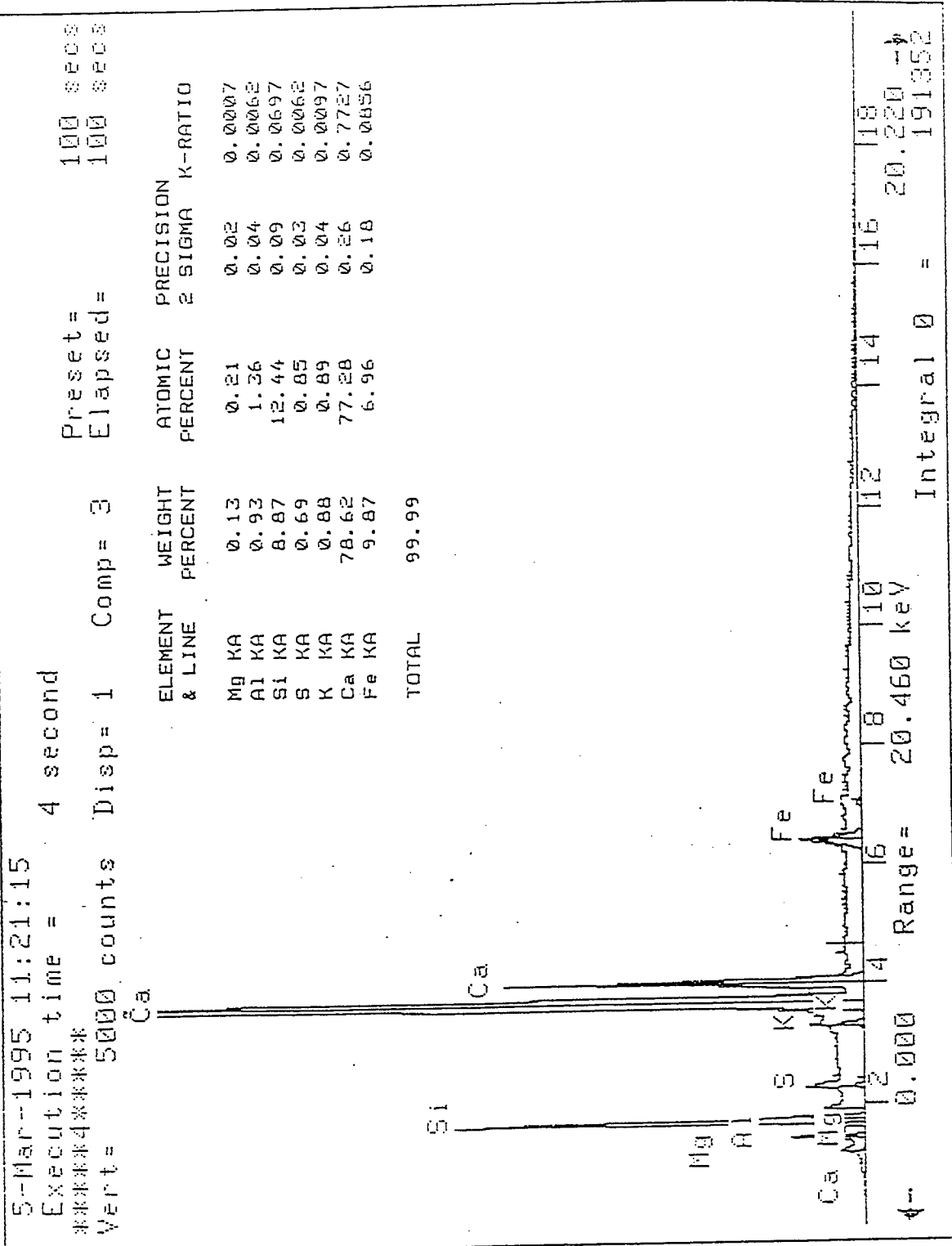


Figure 33. EDS spectrum of sample S-4 of cement-silica fume paste.

7-Mar-1995 09:27:16

Execution time = 4 second

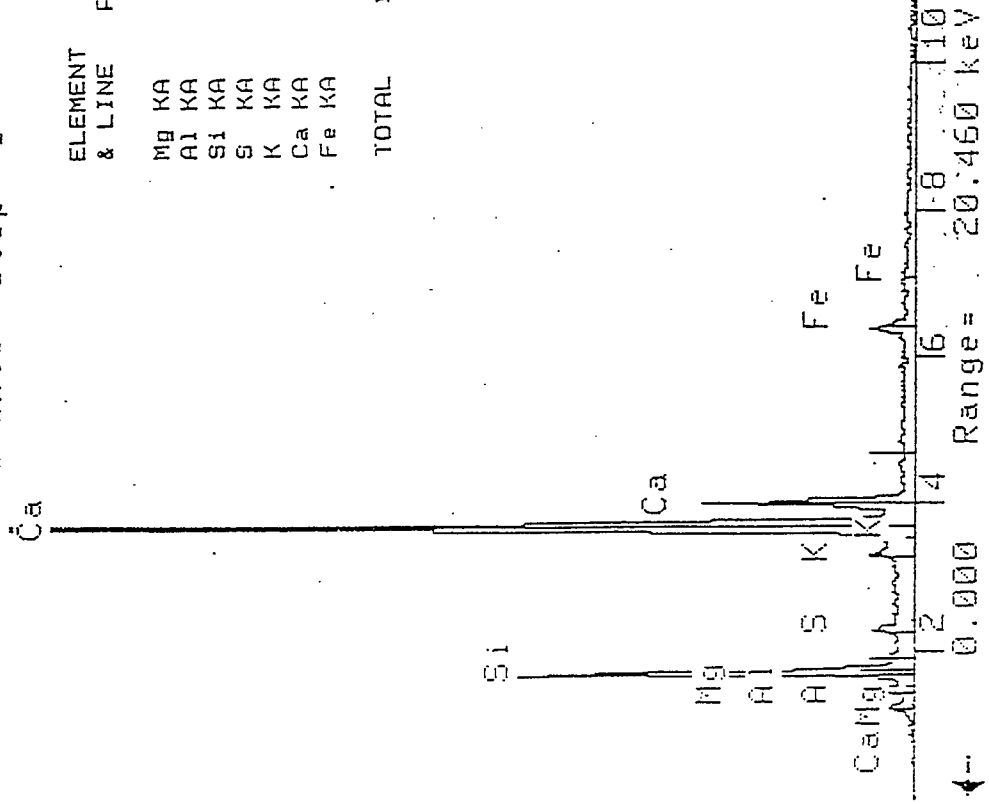
*****5*****

Vert = 5000 counts Disp = 1

Preset = 100 secs

Elapsed = 100 secs

ELEMENT & LINE	WEIGHT PERCENT	ATOMIC PERCENT	PRECISION 2 SIGMA	K-RATIO
Mg KA	0.49	0.77	0.04	0.0027
Al KA	1.10	1.57	0.06	0.0074
Si KA	13.22	18.15	0.14	0.1045
S KA	0.69	0.83	0.05	0.0060
K KA	1.18	1.16	0.06	0.0125
Ca KA	73.61	70.81	0.35	0.7168
Fe KA	9.71	6.70	0.24	0.0841
TOTAL	100.00			



Integral 0 = 103621

Figure 34. EDS spectrum of sample S-5 of cement-silica fume paste.

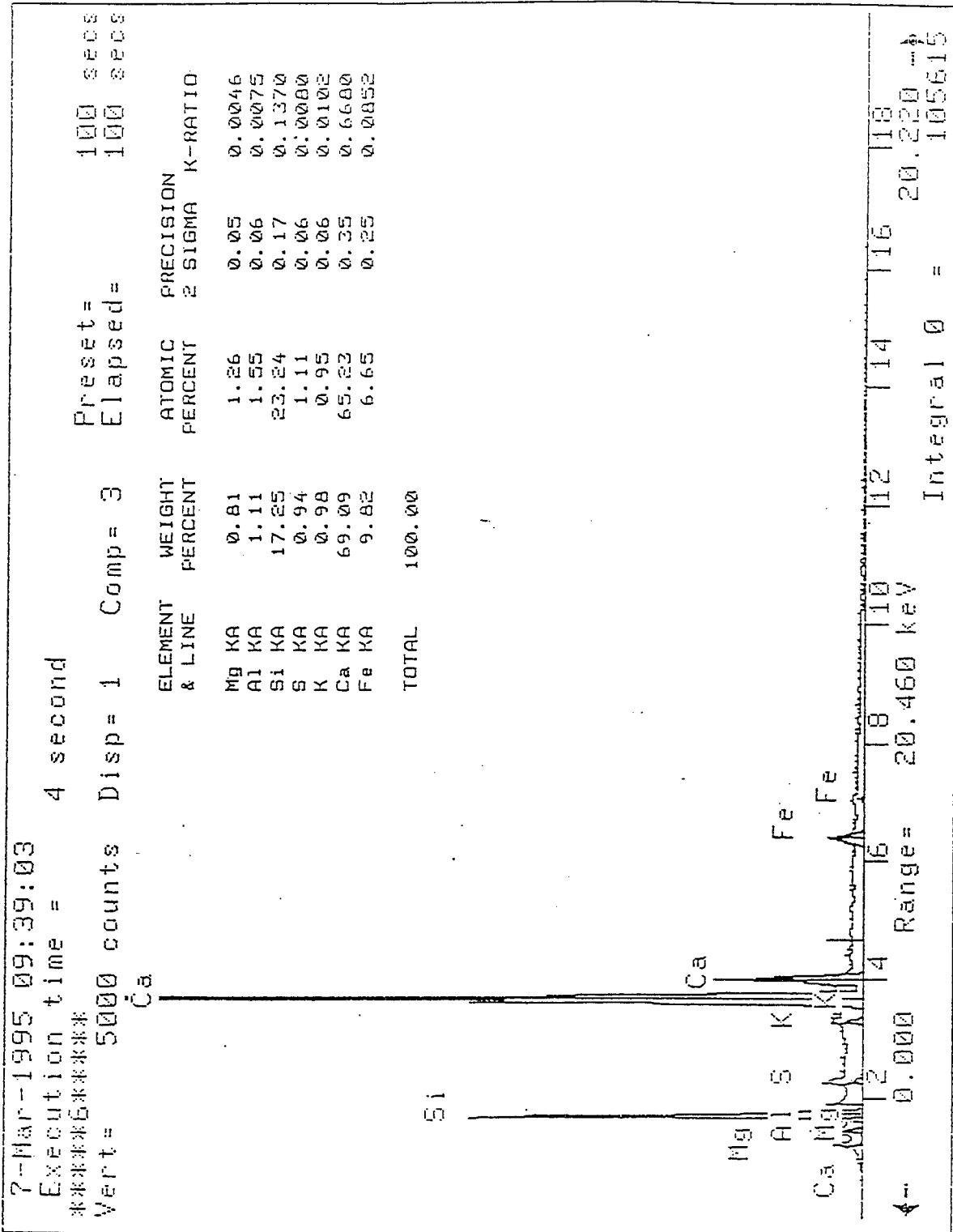


Figure 35. EDS spectrum of sample S-6 of cement-silica fume paste.

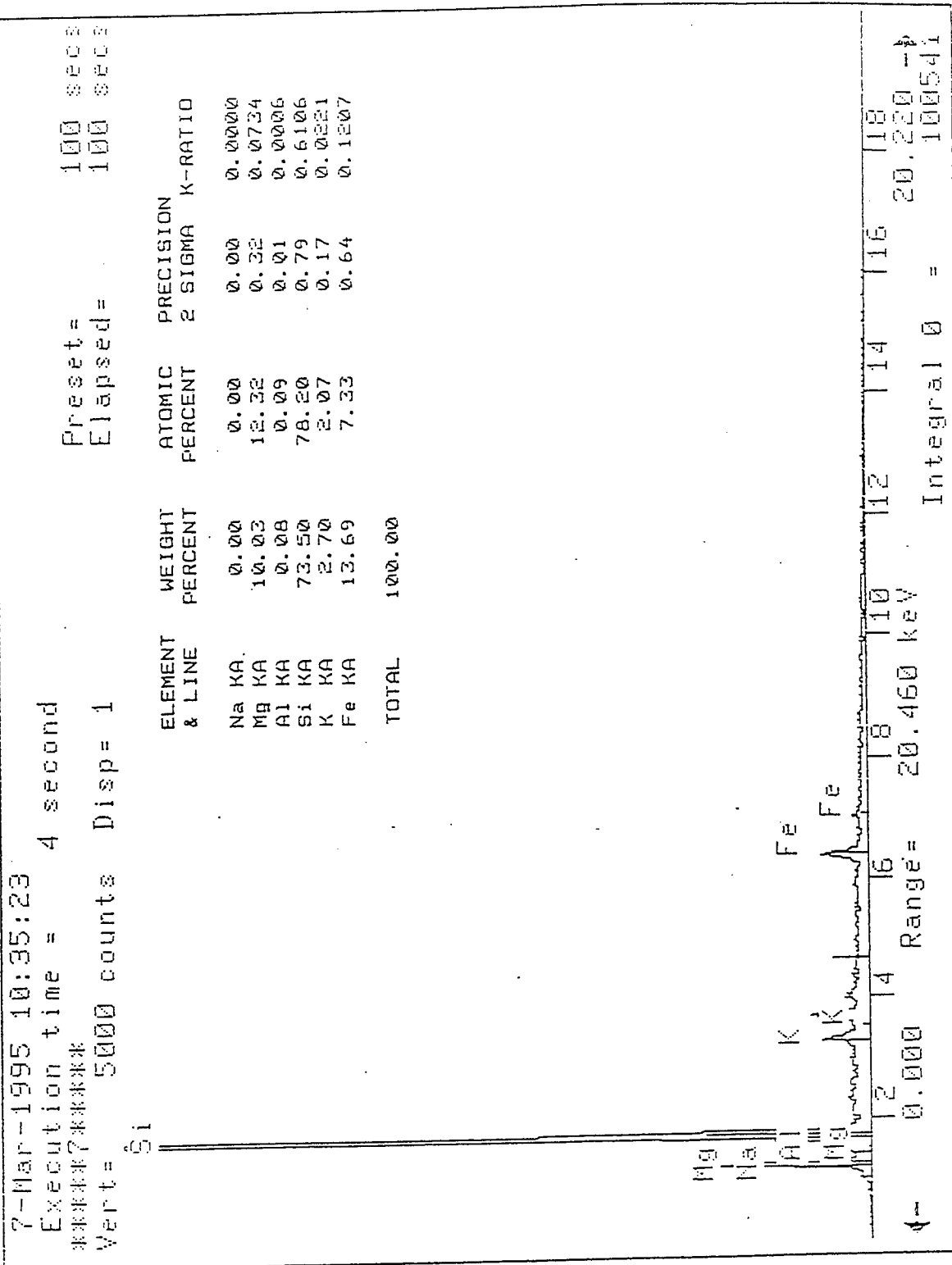


Figure 36. EDS spectrum of sample S-7 of cement-silica fume paste.

NTIS does not permit return of items for credit or refund. A replacement will be provided if an error is made in filling your order, if the item was received in damaged condition, or if the item is defective.

Reproduced by NTIS

National Technical Information Service
Springfield, VA 22161

*This report was printed specifically for your order
from nearly 3 million titles available in our collection.*

For economy and efficiency, NTIS does not maintain stock of its vast collection of technical reports. Rather, most documents are printed for each order. Documents that are not in electronic format are reproduced from master archival copies and are the best possible reproductions available. If you have any questions concerning this document or any order you have placed with NTIS, please call our Customer Service Department at (703) 487-4660.

About NTIS

NTIS collects scientific, technical, engineering, and business related information — then organizes, maintains, and disseminates that information in a variety of formats — from microfiche to online services. The NTIS collection of nearly 3 million titles includes reports describing research conducted or sponsored by federal agencies and their contractors; statistical and business information; U.S. military publications; audiovisual products; computer software and electronic databases developed by federal agencies; training tools; and technical reports prepared by research organizations worldwide. Approximately 100,000 *new* titles are added and indexed into the NTIS collection annually.

For more information about NTIS products and services, call NTIS at (703) 487-4650 and request the free *NTIS Catalog of Products and Services*, PR-827LPG, or visit the NTIS Web site
<http://www.ntis.gov>.

NTIS

*Your indispensable resource for government-sponsored
information—U.S. and worldwide*



U.S. DEPARTMENT OF COMMERCE
Technology Administration
National Technical Information Service
Springfield, VA 22161 (703) 487-4650
